

## ABSTRACT

### THE EFFECT OF LANDSCAPE PATTERN AND VEGETATION COVER TYPES ON THE FIRE REGIME OF A SAVANNA IN SOUTHERN MALI

By

Aurahm Jo

January 2016

Understanding the causes of specific fire regimes is critical for determining the long term impacts of fire on vegetation cover. Numerous studies using 30 m Landsat data find a relationship between fire timing and vegetation type, but this relationship has not been observed at broader scales. In West Africa land-cover patterns are heterogeneous and patchy at the landscape scale and annual fires often burn mosaic patterns. It is well documented that where fires are known to be small and fragmented, the commonly used coarse-resolution MODIS data cannot give accurate estimates of burned area. Moreover, their inability to capture the spatial pattern of land-cover types burned presents a mixed pixel problem, because vegetation and agricultural fields vary on a scale less than 500 m<sup>2</sup>. To overcome these issues, this study uses medium-resolution Landsat data to map land-cover. Landscape ecological indices are used to observe spatial patterns at 500 m scale.

THE EFFECT OF LANDSCAPE PATTERN AND VEGETATION COVER TYPES ON  
THE FIRE REGIME OF A SAVANNA IN SOUTHERN MALI

A THESIS

Presented to the Department of Geography  
California State University, Long Beach

In Partial Fulfillment  
of the Requirements for the Degree  
Master of Arts in Geography

Committee Members:

Paul Laris, Ph.D. (Chair)  
Suzanne P. Wechsler, Ph.D.  
Christine M. Rodrigue, Ph.D.

College Designee:

Rebekha Abbuhl, Ph.D.

By Aurahm Jo

B.A., 2013, University of North Carolina, Chapel Hill

January 2016

WE, THE UNDERSIGNED MEMBERS OF THE COMMITTEE,  
HAVE APPROVED THIS THESIS

THE EFFECT OF LANDSCAPE PATTERN AND VEGETATION COVER TYPES ON  
THE FIRE REGIME OF A SAVANNA IN SOUTHERN MALI

By

Aurahm Jo

COMMITTEE MEMBERS

---

Paul Laris, Ph.D. (Chair)

Geography

---

Suzanne P. Wechsler, Ph.D. Geography

---

Christine M. Rodrigue, Ph.D. Geography

ACCEPTED AND APPROVED ON BEHALF OF THE UNIVERSITY

---

Rebekha Abbuhl, Ph.D.  
Director of Graduate Studies

California State University, Long Beach

January 2016

Copyright 2016

Aurahm Jo

ALL RIGHTS RESERVED

## TABLE OF CONTENTS

|   | Page |
|---|------|
| LIST OF TABLES .....  | iv   |
| LIST OF FIGURES .....                                       | v    |
| CHAPTER   |      |
| 1. INTRODUCTION .....                                       | 1    |
| 2. METHODS .....  | 7    |
| Study Area .....  | 7    |
| Fire Regime Data .....                                      | 9    |
| Landsat Processing.....                                     | 10   |
| Landsat Data Aggregation .....                              | 11   |
| MODIS Burned Area Processing.....                           | 13   |
| MODIS Active Fire Processing .....                          | 13   |
| Land-cover Data.....  | 16   |
| Statistical Test.....                                       | 16   |
| 3. RESULTS .....  | 23   |
| Comparing Average Burned Dates from Landsat and MODIS ..... | 23   |
| Landsat Fire Regime .....                                   | 24   |
| Landscape Indices .....                                     | 29   |
| 4. DISCUSSION .....   | 37   |
| REFERENCES .....  | 43   |

## LIST OF TABLES

| TABLE  | Page |
|--|------|
| 1. Descriptions of Class-Level Indices and Landscape-Level Indices ..... | 19   |
| 2. FRAGSTATS Results for Class-Level Indices.....                        | 21   |
| 3. FRAGSTATS Results for Landscape-Level Indices .....                   | 22   |
| 4. Descriptive Statistics for Class-Level Indices .....                  | 30   |

## LIST OF FIGURES

| FIGURE  | Page |
|---|------|
| 1. Study area.....  | 7    |
| 2. Calculating average fire dates, fire frequency, and standard deviation of fire dates for MODIS active fire dataset.....  | 15   |
| 3. Land-cover map (30 m) .....  | 17   |
| 4. Scales of landscape indices .....  | 18   |
| 5. Box plots of burned dates (500 m pixel) by dataset.....  | 24   |
| 6. Box plots of average burned dates for 1 <sup>st</sup> and 4 <sup>th</sup> quartile of percentage cover of (a) short grass savanna, (b) agriculture/short fallow, (c) savanna/long fallow, and (d) woodlands.....         | 25   |
| 7. Box plots of burn frequency for 1 <sup>st</sup> and 4 <sup>th</sup> quartile of percentage cover of (a) short grass savanna, (b) agriculture/short fallow, (c) savanna/long fallow, and (d) woodlands.....               | 26   |
| 8. Box plots of variability of burned dates for 1 <sup>st</sup> and 4 <sup>th</sup> quartile of percentage cover of (a) short grass savanna, (b) agriculture/short fallow, (c) savanna/long fallow, and (d) woodlands ..... | 28   |
| 9. Short grass savanna.....   | 31   |
| 10. Agriculture/short fallow.....   | 32   |
| 11. Savanna/long fallow.....  | 33   |
| 12. Woodlands .....   | 34   |
| 13. Landscape .....   | 35   |

## CHAPTER 1

### INTRODUCTION

Savannas are a unique biome, defined by a coexistence of grasses and scattered trees (Scholes and Archer 1997). African savannas are the most frequently and extensively burned regions in the world (Giglio et al 2010). From an ecological standpoint, fires in savannas are not only normal, but necessary. Frequent disturbances, such as fires or grazing, temporarily lead to favorable conditions for trees or grasses, preventing one plant type from outcompeting the other (Jeltsch et al 2000; Laris 2011; Sankaran et al 2005). Fires also have climatic impacts (Archibald et al 2010). They emit greenhouse gases such as carbon dioxide, methane, nitrous oxide, and particulates (Koppman et al 2005), cause vegetation cover changes (Louppe et al 1995), and suppress growth of woody vegetation, which stores carbon (Bond et al 2005).

Responding to the rising concerns over fires in African savannas, many studies have focused on identifying drivers of fire regimes. The fire regime of an area is defined by its type, intensity, size, return interval, seasonality, and spatial pattern (Christensen 1985; Agee 1993; Bond and Keeley 2005). Major drivers can be clustered into four categories: landscape pattern, anthropogenic factors, weather and climate, and fuel structure and flammability. Landscape variables defining composition (land-use and land-cover type) or proximity to human influence affect fire occurrence and patterns (Moreno et al 2011). The intermixing of woodland and agricultural land has been shown

to influence a fire regime because agricultural fields can act as firebreaks (Lloret et al 2002; Loepfe et al 2010, 2011). Fires have differentially burned certain land-use and land-cover types in the Mediterranean (Moreira et al 2001, 2009; Nunes et al 2005; Bajocco and Ricotta 2008), as well as in other regions (Cumming 2001; Vázquez and Moreno 2001; Mermoz et al 2005).

Interannual climate variation or meteorological patterns are important determinants of yearly burned area or fire-size patterns in many environments (Littell et al 2009; Lutz et al 2009; Sá et al 2010). There is a growing concern that climate change will cause larger and more catastrophic fires around the world.

Anthropogenic factors including fuel fragmentation, fire suppression, population density, agriculture proportion, and exotic species play a major role influencing fire regimes throughout the world (Brown et al 2004; Duncan and Schmalzer 2004; Martinez et al 2009; Sá et al 2010). Fuel structure and flammability have been proposed as alternative drivers of fire regimes especially in California shrublands (Minnich 1983; Keeley et al 1999; Keeley and Zedler 2009). While fuel moisture determines plant flammability (availability to burn), fuel structure refers to the amount and connectivity of burnable resources. Some authors claim that a reduced number of small and mid-sized fires result in an accumulation of fuel that may lead to catastrophic fires under extreme weather conditions (Pausas and Paula 2012; Minnich 1983, 2001; Piñol et al 2005, 2007; Shang et al 2007). Others hold that, in some ecosystems at least, large fires are not dependent on the age classes of fuels (Loepfe et al 2011; Moritz 2003; Moritz et al 2004). The spatiotemporal patterns of fires themselves can influence fire behavior and burned area. As several authors have shown, a regime of patch or seasonal mosaic fires creates a

landscape fragmented by early and late fires that prevents large sweeping fires and has specific ecological and management benefits (Laris 2011; Parr and Brocket 1999).

Fire is thus a landscape-scale phenomenon that depends on connectivity of a flammable fuel load across space and time. In savanna ecosystems, the fire regime strongly affects tree establishment and growth: in particular, the timing of fires is a critical determinant of fire intensity and its impact on trees (Louppe et al 1995; Furley et al 2008). In areas such as the African savannas, which have high fire frequency, landscape and fire patterns are changing continuously over time, making fire mapping a challenge. Remote sensing offers one of the few means to provide accurate data on savanna fire regimes.

While global fire products are widely available and provide timely data on African fire regimes, they are not without serious inaccuracies. Because of the highly fragmented landscape in savannas, scale of analysis is critical in detecting the spatiotemporal patterns of burning in savannas. Researchers have often relied on global products derived from Moderate Resolution Imaging Spectroradiometer (MODIS), whose high temporal resolution (daily) is offset by coarse spatial resolution (500 m or 1 km) (e.g., Archibald et al 2009, 2010; Sá et al 2010). In savannas, where fire is a frequent and widespread phenomenon, use of coarse-resolution products poses a trade-off for analysts: while most fires larger than the pixel resolution are mapped, those smaller are most often missed. This phenomenon is known as “low-resolution bias” (Boschetti et al 2004, 2013). As Laris (2005) demonstrated, use of coarse-resolution data is problematic in African savannas where early-season fires tend to be fragmented and smaller than the pixel size. MODIS burned area data may further underestimate burned areas because of

the conservative algorithm used to create the data product: partially burned pixels are classified as unburned (Boschetti et al 2013; Laris 2005). Finally, as Randerson et al (2012) demonstrated, the error associated with the burned area products for African savannas is large. MODIS active fire data also underestimate the number and size of fires, as the satellite may not pass over when the burning occurs. Further, even if satellite timing is ideal, active fires may not be detected because of clouds or optically thick smoke (Giglio 2007, Roy et al 2008, Smith and Wooster 2005), or if fires are too small or not hot enough (Giglio et al 2003, Schroeder et al 2008). Active fire detections have been found to underestimate burned areas in savannas where fires progress rapidly across the landscape (Boschetti and Roy 2009; Roy et al 2008).

Compounding these issues in many savannas is burning patterns created by people: such patterns are highly fragmented and can be undetectable using coarse-resolution data. When rural inhabitants in savannas set fires, they tend to make decisions at a landscape scale (on the order of hectares) because vegetation varies at this scale (Laris 2011; Duvall 2011). Laris (2005) compared the burned area estimates of Landsat data at the 30 m pixel to products (SPOT-Vegetation and ATSR) derived from coarse-resolution satellites at the 1 km pixel, finding that Landsat data show a significantly higher percentage of the study area burned. Caillault et al (2014) found similar results for Burkina Faso.

Additionally, MODIS data are likely to be subject to mixed pixel problems. Though daily MODIS data are readily available with vegetation types already classified, changes in land-cover types, unlike burned area, do not occur daily. Therefore, for land-cover mapping, sacrifice of spatial resolution for temporal resolution often is not

appropriate. Land-cover types are much more difficult to determine accurately at the 500 m or 1 km pixel of MODIS than at the 30 m pixel (such as with Landsat); multiple types of land cover might be included but not differentiated in a single MODIS pixel.

In complex and heterogeneous landscapes such as a savanna (Duvall 2011), landscape pattern can play a critical role in determining the spatiotemporal patterns of fire; therefore, landscape ecological indices should hold potential for linking land-cover patterns to fire regimes. As has been demonstrated, landscape pattern plays a critical role in determining whether and how a fire burns through a landscape—a classic case of pattern influencing ecological process (Turner 1989; McGarigal 2015; Midha and Mathur, 2010; Raines 2002).

Landscape indices, developed to quantify ways in which pattern affects ecological processes (Pickett and White 1985, Turner 1989), help to show the relationship between landscape patterns and fire regime dynamics. Landscape characteristics are spatially variable, and fire spread is not independent of them (Moreno et al 2011). In helping to quantify relationships between landscape characteristics and fire regimes, landscape indices can be used to consider elements within a 500 m block, such as a MODIS pixel, as related or spatially dependent.

The purpose of this thesis is to analyze the effects of vegetation types and their landscape patterns on the three key parameters of the fire regime—timing, frequency, and variability of fires in southern Mali.

The study is driven by four key research questions:

1. How does landscape pattern affect the fire regime in an African savanna?

2. Do particular types of vegetation cover (e.g., short grass savanna or rotational agriculture) have unique effects on specific aspects of the fire regime?

3. Which common landscape ecological indices have the most potential for linking land cover and fire regime?

4. What potential do landscape indices offer for resolving the issue of scale in use of coarse-resolution fire and land-cover data?

To address these questions, my approach expanded upon earlier efforts to link fire regimes to land use and cover in savannas. First, a unique data set was developed by combining MODIS and Landsat data. Use of both sources contributed to a more robust set of data to analyze the fire regime: daily MODIS data provide accurate temporal information, and less frequent Landsat data with higher spatial resolution improve classification accuracy of primary determinants (type and pattern of vegetation and land cover). Second, landscape indices were used to characterize vegetation patterns for each 500 m MODIS pixel by co-locating patches of 30 m pixels of classified Landsat data and transforming them into landscape indices to characterize the spatial pattern. Third, to better understand dynamics of landscape patterns over time, a typology of landscape forms was created by identifying vegetation type (short grass savanna, agriculture/short fallow, savanna/long fallow, and woodlands). Finally, relationships between key factors (vegetation type, pattern of agriculture, landscape indices) and the fire regime in southern Mali were examined to test the first tenet of landscape ecology—*spatial patterns of the landscape affect ecological processes* (Turner 1989)— and to better understand the fire regime.

## CHAPTER 2

### METHODS

#### Study Area

The study area is located in southern Mali and northern Guinea, the southern edge of the Soudan savanna belt (Figure 1). Its spatial extent corresponds to the Landsat scene WRS-199/52 (Lon:  $-7^{\circ} 17'$ -  $-9^{\circ} 2'$ , Lat:  $10^{\circ} 41'$ - $12^{\circ} 28'$ ). The study area ( $32,927 \text{ km}^2$ ) is contained within this scene boundary and is smaller than the boundary because of scene shifting over the 11-year study period.

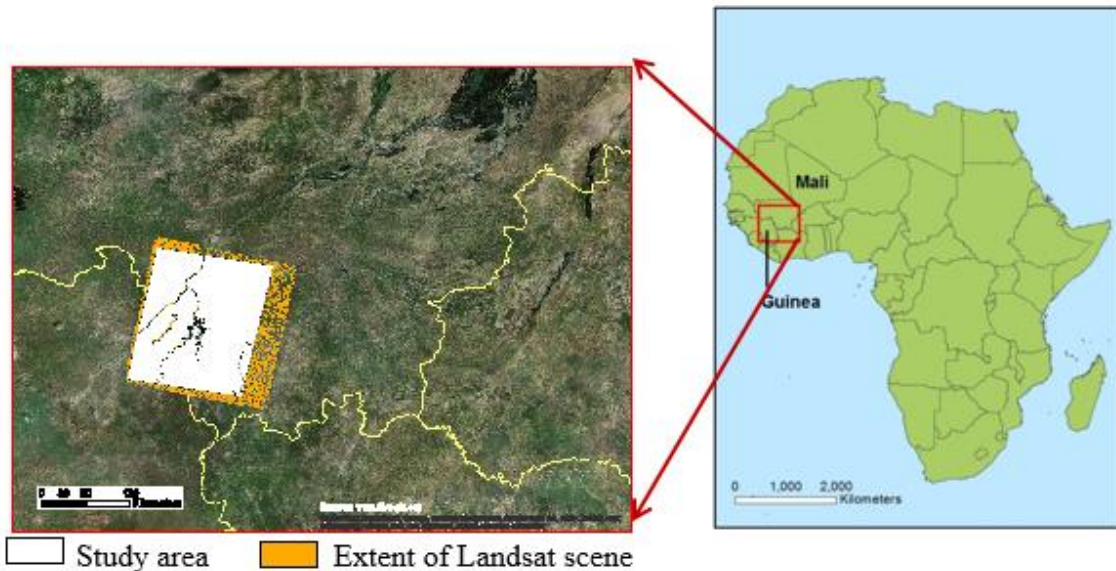


FIGURE 1. Study area. The study area falls within the spatial extent of a Landsat scene (199/52) that borders Guinea and Mali (ESRI 2009).

This region is a mesic savanna with an average annual rainfall between 1,000 and 1,200 mm (Nasi and Sabatier 1988) and relatively cool and hot dry seasons characterized by fires: a cooler dry season from October to February and a hot and dry season from February to June. The dry season is followed by a rainy season that runs from June to October. Although rainfall is sufficient to support the growth of closed canopy tree cover, disturbances such as fires adversely impact their development. People set fires to the landscape to protect their agricultural fields from larger fires. Where and when fires are set is determined by the vegetation (Laris 2002).

The vegetation in this study area is categorized as southern Soudanian savanna and comprised mainly grasses, trees, and shrubs. Agricultural fields left fallow for short period of time (less than five years) are mainly composed of annual grasses mixed with frequently farmed fields (Laris 2013). Short grass savannas are dominated by short annual grasses with few widely scattered trees (Nasi and Sabatier 1988). Because short grass savannas grow on poor soils, they are not cultivated. Fires are set in these short grasses earlier in the fire season because they are the first to dry and have uneven distribution throughout the landscape. Thus, fires in these short grasses are small and are naturally extinguished when they reach vegetation that is not as dry. These early fires protect the more productive agricultural lands from larger fires because an area typically burns only once in a season.

More fertile soils are characterized by more dense woody vegetation and tall perennial grasses, which hold more moisture than the annuals. Perennial grasses also grow in agricultural areas that have been left fallow for a long time (longer than five years). Agriculture in these areas tends to take place once the vegetation has been fallow

for a sufficient period of time (longer than five years). To fragment the landscape and prevent larger fires, areas containing taller perennial grasses, are burned before harvest in the agricultural areas. Woodlands are the last to burn because trees hold the most moisture, but only juveniles burn because fully grown trees become immune to the low-intensity fires.

#### Fire Regime Data

Because the fire regime markedly affects tree establishment and growth in savanna ecosystems, timing of fires is especially important. Fire intensity increases as the season progresses and vegetation dries. In this research, data were obtained from October to May. Although the dry season lasts until June, fires typically do not occur so late in the season, so data for June were not included. The data used in this research were obtained from Landsat imagery (2002, 2006, and 2013), MODIS burned area imagery (2003-2014), and MODIS active fire point data (2003-2014).

Variables used to characterize the fire regime were derived from all three data sources: (1) timing of the fire; (2) frequency of the fire; and (3) variance of average burn date. The unit of analysis is the 500 m pixel (250,000 m<sup>2</sup>) of the MODIS burned area data. Each Landsat pixel has a resolution of 30 m (900 m<sup>2</sup>); Landsat data were aggregated to the spatial extent of the 500 m MODIS pixels.

All of the datasets provide burned dates as Julian days. Each dataset was modified, setting October 1<sup>st</sup> to 1 to indicate the start of the season (rather than January 1<sup>st</sup>). The largest possible value was set to 243 or May 31<sup>st</sup>, which was selected as the end of each fire season.

In MODIS data there are two major fire detection methods—burned area and active fire. Burned area products are created using a burned area detection method, which delineates burned areas by detecting spectral contrast between vegetation modified by fires and vegetation unaffected by fires. A reflectance threshold is set to distinguish burned and unburned areas. Active fires are mapped by detecting the thermal signature or high temperature of the flaming front of a fire.

Each dataset has a different range of burn frequency values. For all datasets, a pixel typically burns once in a season, so MODIS datasets theoretically have a maximum frequency value of 11. A small number of cells in these datasets burned more than once, resulting in values of 13 (MODIS burned area) and 12 (MODIS active fire). Landsat can have a maximum frequency of 300 because 100 50 m pixels fit within a 500 m pixel, meaning that for each season, a 500 m pixel can experience 100 individual burns; we have three seasons of fire data for Landsat. Estimating the average burned date per 500 m pixel required two steps: (1) Landsat data processing to create burned area maps and (2) data aggregation.

### Landsat Processing

Landsat images cover three fire seasons: 2002, 2006, and 2013. Data for the first two were created using Landsat 4 Thematic Mapper (TM) and Landsat 7 Enhanced Thematic Mapper Plus (ETM+) images by Laris (2013). For the most recent fire season, images from TM and Landsat 8 Operational Land Imager and Thermal Infrared Sensor (OLI and TIRS) were used. The TM, ETM+, and OLI imagers provide identical bandwidths and pixel resolutions, enabling long-term monitoring.

The Landsat burn scar maps, which contain burn date information, were combined into one image from which average burned dates, burn frequency, and standard deviation of burned dates were derived. The burned area maps were created as follows (Laris 2011):

- 1) Using ENVI version 5.0 (Exelis Visual Information Solutions, Boulder, Colorado), an unsupervised clustering algorithm (ISODATA) was applied to six bands of Landsat images (2-7 for OLI; 1-5 and 7 for TM and ETM+). The clustering algorithm grouped 30 m pixels into 25 spectral classes.
- 2) Each class was visually assessed as either burned or unburned by comparing to a false-color image (5-4-3 band combination).
- 3) Pixels burned in prior months were removed, since areas burned once during the fire season typically do not burn again, although the burn scar may remain visible. This approach resulted in one 30 m resolution image per season.
- 4) A  $4 \times 4$  majority filter was applied to remove lone pixels, i.e. those different from adjacent pixels; and
- 5) water bodies were masked. Each 30 m pixel was identified as either burned or unburned. The burned pixels contain the numerical burn date value (Julian dates were reassigned so that October 1<sup>st</sup> became “1” with a maximum date of 243 corresponding to May 31).

#### Landsat Data Aggregation

The three 30 m Landsat images containing the burn date information on a per-pixel-basis were aggregated into three 500 m images corresponding to the footprint of the MODIS dataset. The average, frequency, and standard deviation images were generated as follows:

Frequency image: Each Landsat image was resampled to 50 m (using the resample tool in ArcGIS). A value of 1 was assigned to each burned area pixel. This 50

m binary frequency image was used to derive a 500 m frequency image, using block statistics whereby the 500 m pixel was attributed with the sum of the burned areas in the corresponding 100 pixels from the 50 m input image. The resulting three frequency images at 500 m resolution, corresponding to the 2002, 2006 and 2013 Landsat seasons, were summed to yield a total frequency image at 500 m resolution.

Average image: Each Landsat image was resampled to 50 m (using the resample tool in ArcGIS) using nearest-neighbor interpolation method. Each 50 m pixel has a burned date value or zero for unburned pixels. This 50 m burned date image was used to derive a 500 m total burn date image, using block statistics whereby the 500 m pixel was attributed with the sum of the burned dates in the corresponding 100 pixels from the 50 m input image. The total burned date for each of the three seasons was summed into a single total burn date image at 500 m resolution. The total burn date was divided by the total frequency image to derive an average burn date image, representing the overall average burn date for the three seasons.

The standard deviation of burned dates for each 500 m aggregate pixel was calculated using equation (1):

$$\sum_{i=1}^n \sqrt{\frac{(X_{burned} - X_{avg})^2}{n-1}} \quad \text{eq (1)}$$

where

$X_{burned}$  = per pixel burned date preprocessed to convert “0” values to “no data”

$X_{avg}$  = average burned date for 500 m pixel resampled to 50 m for calculation purposes

N = frequency for 500 m pixel resampled to 50 m for calculation purposes  
(maximum corresponding to the 100 50 m cells for three seasons)

If the standard deviation of average burn dates per 500 m pixel is small, a pixel would burn around the same time for each fire season. The resulting three grids at 500 m were further summarized to calculate the overall averages of the average burn date, burn frequency, and standard deviation of the burned dates across the entire study area.

#### MODIS Burned Area Processing

MODIS burned area data are provided monthly at 500 m resolution. For each burned pixel, the approximate Julian day of burning is reported. The downloaded images were clipped to the extent of the study area.

The frequency image was calculated by reassigning burned pixels (those containing dates) with a value of 1 and summing all the monthly images for the 11-year period (2003-2014). The average burned date image was calculated by summing all the monthly images with burned dates (Julian dates were reassigned so that October 1<sup>st</sup> became “1” with a maximum date of 243 corresponding to May 31), then dividing by the frequency image. The standard deviation of burned dates image was calculated following equation 1 where

$X_{\text{burned}}$  = per pixel burned date preprocessed to convert “0” values to “no data”

$X_{\text{avg}}$  = average burned date

N = 13 (burn frequency grid)

#### MODIS Active Fire Processing

MODIS active fire data are provided as point shapefiles where each point represents the date of the fire (Julian dates were reassigned so that October 1<sup>st</sup> became

“1” with a maximum date of 243 corresponding to May 31). The points were downloaded and clipped to the study area. A series of spatial joins was required to aggregate the point data to 1 km polygons while retaining the detailed data contained in the original point file (Figure 2). The average, frequency, and standard deviation for MODIS active fire were calculated:

(1) The downloaded and clipped points were converted to an image at a 1 km pixel resolution (corresponding to the resolution of the MODIS active fire imagery). (2) This 1 km image was converted to a polygon shapefile for use in the subsequent spatial joins. (3) The original clipped points were spatially joined to the 1 km polygons, resulting in 1 km<sup>2</sup> polygons with an attribute table containing the sum of the fire dates and frequency of fire dates. From this the average fire date was calculated. If, for example, the sum of the modified Julian dates was 540, and the frequency of burn was 4, the average fire date would be 135 (equivalent to Feb 12). A pixel could have two points for a given day if there were active fires in the morning and afternoon, detected by Terra and Aqua satellites, respectively.

(4) The information derived from this polygon file was then associated with the original clipped point file, using intersect to spatially join the data from the polygon back to the point file. The resulting point file retains the original fire dates but is enhanced with the frequency and average burn date associated with each point. From this information, a difference squared field could be calculated from the modified Julian date and average burn date.

(5) The point shapefile resulting from the spatial join/intersect (step 4) was rejoined to the spatially joined polygons (step 3) resulting in a polygon shapefile that

enabled the calculation of the standard deviation of actual burn date for each 1 km<sup>2</sup> area. In this shapefile, the difference squared field summed during the spatial join process (numerator) and the sum of frequency (denominator) were used to calculate the standard deviation of burn date for each polygon.

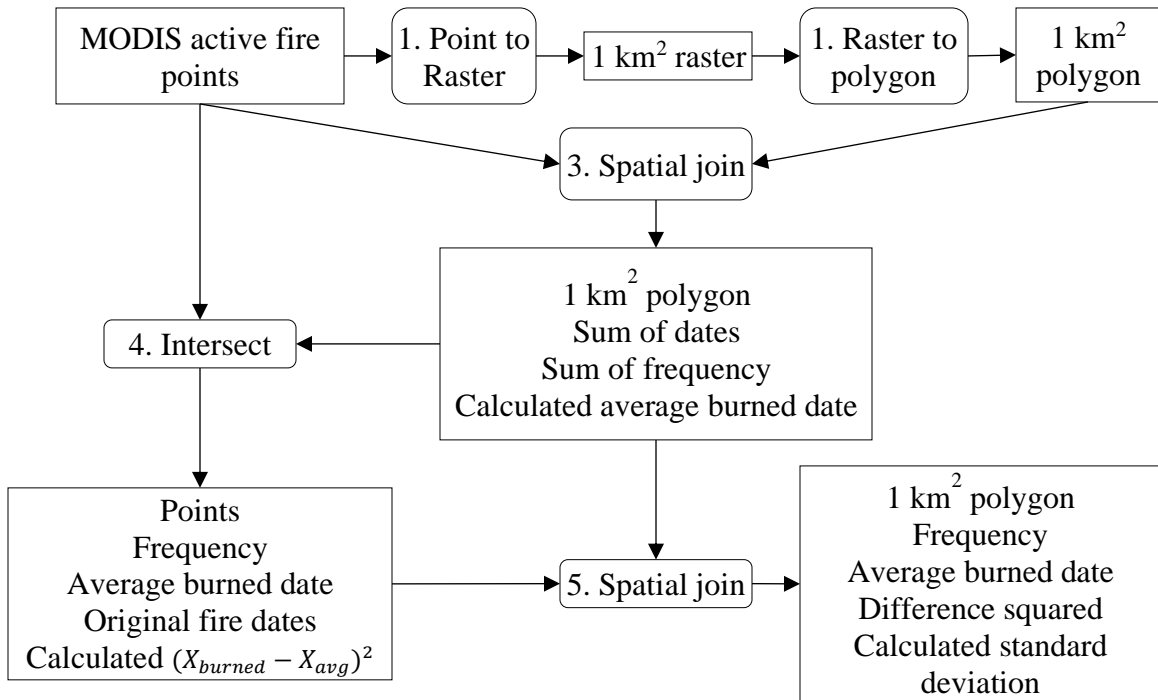


FIGURE 2. Calculating average fire dates, fire frequency, and standard deviation of fire dates for MODIS active fire dataset

(6) The average, frequency, and standard deviation fields in the polygon shapefile (step 5) were converted to 3 image grids at 1 km resolution. (7) These were each resampled to 500 m images to correspond to the MODIS burned area resolution.

### Land-cover data

Selection of appropriate vegetation types that determine the fire regime is based on a conceptualization of the drivers of fire in southern Mali. Drivers include agricultural fields and vegetation type (i.e., woodlands, savanna/long fallow, agriculture/short fallow, and short grass savanna). All are thought to affect spatial extent and seasonality of fires (Laris, 2005; 2011). Though additional environmental factors in previous studies included rainfall, wind speed, and relative humidity at the time of burning, they are not included here because of lack of variation across the study area (e.g., similar quantity of rainfall) and data availability.

The land-cover data used in this analysis were obtained from an image developed by Laris (2011), using three November images from the modern period (2000, 2002, and 2006), and three from the historical period (1986, 1988, and 1991). The land-cover map originally had six land-cover types: (1) water, (2) woodlands, (3), savanna/long fallow, (4) short grass savanna, (5) agriculture/short fallow, and (6) settlements. For the purposes of this analysis, water and settlement classes were excluded because these classes are not flammable (Figure 3). Although agricultural fields are often considered non-flammable, the short grasses that emerge when they are fallow are flammable. Therefore, for the purposes of this analysis, areas in the land-cover dataset classified as agriculture/short fallow were included as flammable.

There are three landscape scales: landscape, class, and patch. For the purposes of this study, “landscape” is used to refer to each MODIS pixel because the unit of analysis for all datasets is the 500 m pixel.

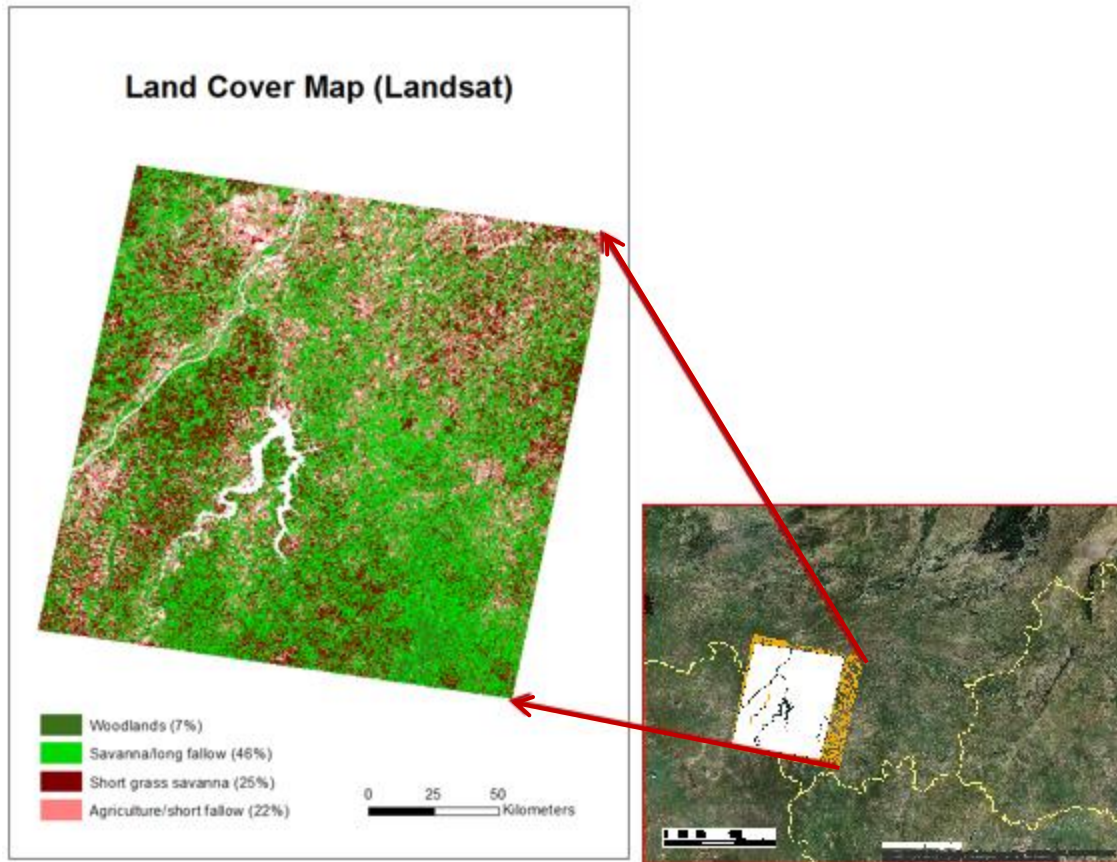


FIGURE 3. Land-cover map (30 m)

The “class” scale is represented by the vegetation type contained in the land-cover dataset. A patch is a group of connected pixels that belong to one vegetation class. For example, in Figure 4, the MODIS pixel with an ID of 1 has only one patch that belongs to a non-flammable class. Figure 4 shows classified, 50 m Landsat pixels within four 500 m MODIS pixels. In this figure, four MODIS pixels (landscape) are shown with the underlying vegetation classes (resampled from the 30 m Landsat to 50 m resolution) and patches become evident.

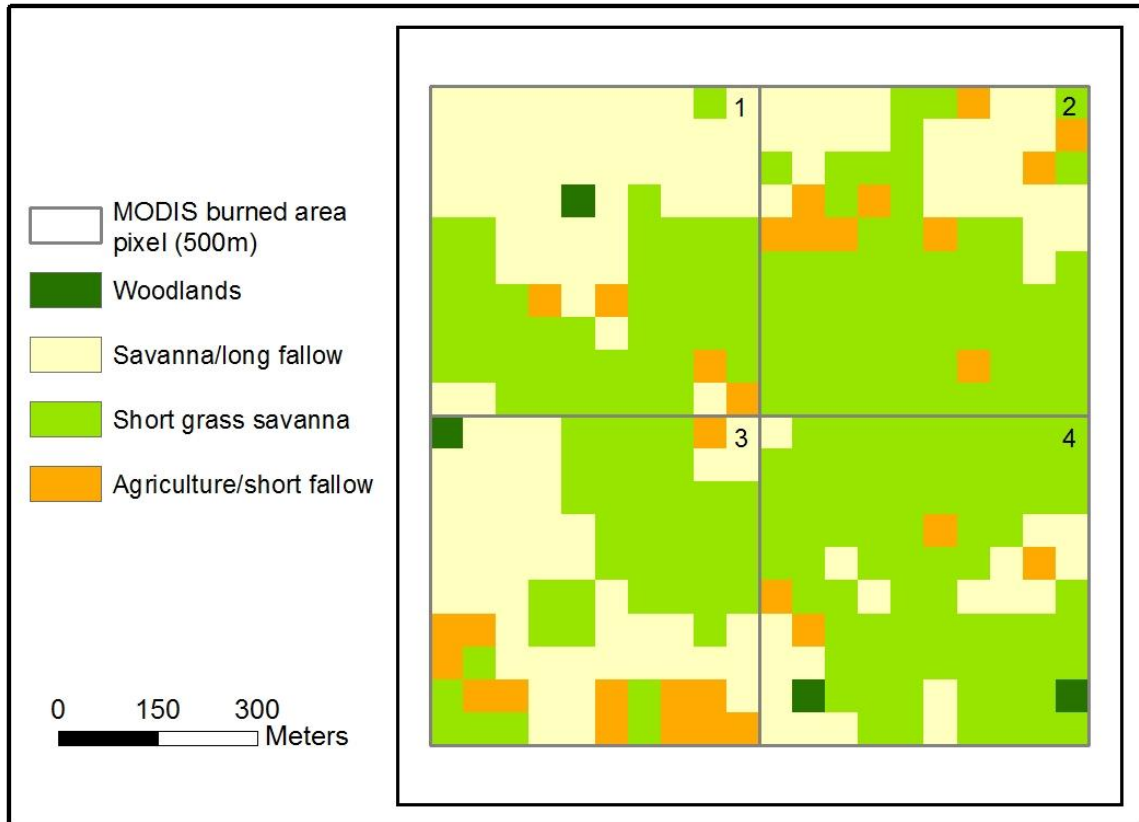


FIGURE 4. Scales of landscape indices. Numbers 1-4 refer to the MODIS 500 m pixel. There are 4 land-cover classes identified from the LANDSAT data at 50 m pixel resolution (resampled from 30 m to 50 m).

Because characterizing the spatial heterogeneity of the various land-cover types within each MODIS pixel could explain why early-season fires tend to be more fragmented than late-season fires in southern Mali, landscape indices were developed to measure the spatial pattern created by the various land-cover types. For each pixel, FRAGSTATS (McGarigal et al 2012) was used to analyze two different levels of spatial pattern metrics: class-level index (CLI) and Landscape-level Index (LLI). The CLI represents the spatial distribution and pattern of a single vegetation type contained in a

MODIS pixel. The LLI calculates a numeric value for the spatial pattern created by all the vegetation types present within a MODIS pixel.

In both the CLI and LLI, four landscape indices were calculated (Table 1).

TABLE 1. Descriptions of Class-Level Indices and Landscape-Level Indices

| Indices  | Explanation   |
|--|---|
| <b>CLI (short grass savanna, agriculture/short fallow, savanna/long fallow, woodlands)</b> |   |
| Proportion of area   | <i>Proportion of landscape area</i> for each vegetation type was calculated as a simple measure of amount of area covered by each vegetation type   |
| Shape index  | <i>Shape index</i> measures shape complexity of a patch compared to a square shape of the same size   |
| Largest patch index  | <i>Largest patch index</i> is the percentage of the total landscape area occupied by the largest patch of a class   |
| Patch density  | <i>Patch density</i> is the number of patches in a land-cover type per 100 hectares.  |
| <b>LLI (all vegetation types)</b>  |   |
| Largest patch index  | <i>Largest patch index</i> is calculated to note the size of largest patch in the landscape regardless of vegetation type   |
| Patch richness   | <i>Patch richness</i> is simply the number of land-cover types present in the landscape.  |
| Splitting index  | <i>Splitting index</i> is equal to 1 when the landscape consists of a single patch. Splitting index increases as the landscape is increasingly subdivided into smaller patches and achieves its maximum value when the landscape is maximally subdivided; that is, when every cell is a separate patch. |
| Patch density  | <i>Patch density</i> is calculated to note the number of patches in a landscape.  |

In the CLI these included (1) proportion of area; (2) shape index; (3) largest patch index; and (4) patch density. In the LLI these included: (1) largest patch index; (2) patch richness; (3) splitting index; and (4) patch density (McGarigal 2015).

In the CLI the *proportion of landscape area* for each vegetation type was calculated as a simple measure of amount of area covered by each vegetation type. *Shape*

*index* measures shape complexity of a patch compared to a square shape of the same size. The *largest patch index* is the percentage of the total landscape area occupied by the largest patch of a class. *Patch density* is the number of patches in a land-cover type per 100 hectares.

In the LLI the *largest patch index* refers to the percentage of landscape area covered by the largest patch in the 500 m pixel, regardless of the vegetation type. *Patch richness* is simply the number of land-cover types present in the landscape; this metric was selected to note the diversity of land-cover types present in each 500 m pixel, regardless of the size or shape of the patches. *Splitting index* is equal to 1 when the landscape consists of a single patch. Splitting index increases as the landscape is increasingly subdivided into smaller patches and achieves its maximum value when the landscape is maximally subdivided; that is, when every cell is a separate patch. *Patch density* is calculated to note the number of patches in a landscape.

To allow the boundaries of the MODIS burned area pixels and Landsat pixels to match, the land-cover map was resampled from 30 to 50 m resolution. Subsequently, the 50 m land-cover map was used as input for FRAGSTATS. In FRAGSTATS, the uniform tiles method was used with a tile side length of 500 m corresponding to the MODIS burned area pixels. The desired LLI and CLI were selected for processing in FRAGSTATS, resulting in two text files and one image (with the tile id information). The text files summarize the class level (short grass savanna, agriculture/short fallow, savanna/long fallow, and woodlands; Table 2) and landscape-level indices (all vegetation in the pixel; Table 3). The tile ID (from MODIS) was used to join the CLI and LLI indices to each MODIS pixel.

TABLE 2. FRAGSTATS Results for Class-Level Indices

| Tile ID | Type        | Percentage cover | Shape index | Largest patch index | Patch density |
|---------|-------------|------------------|-------------|---------------------|---------------|
| 1       | Savanna     | 9%               | 1.83        | 9%                  | 4.07          |
| 1       | Woodlands   | 4%               | 1.00        | 4%                  | 4.07          |
| 1       | Agriculture | 6%               | 1.00        | 6%                  | 4.07          |
| 2       | Savanna     | 11%              | 1.12        | 4%                  | 16.31         |
| 2       | Short grass | 8%               | 1.00        | 6%                  | 8.15          |
| 2       | Woodlands   | 15%              | 1.62        | 15%                 | 4.07          |
| 2       | Agriculture | 4%               | 1.00        | 2%                  | 8.15          |

Each pixel could have a maximum of 5 cover types (i.e., 3 cover types are in MODIS pixel 1 in Table 2). For each, there are four indices (i.e., percentage cover, shape index, largest patch index, and patch density for Table 2). MODIS pixel 1 in Tables 2 and 3 has three cover types, so there are 12 CLIs and 4 LLIs for this pixel. Spatial information was assigned to the information contained in text files by converting the tile id image to points and joining the text files to the points by tile id. Five copies of the point shapefile were created to join each of the landscape and four land-cover types to tile id points separately. Table 2 shows CLI values for two MODIS pixels. Because there are multiple rows of information for a single MODIS pixel, the CLI text file generated by FRAGSTATS was separated by vegetation type and each of the four vegetation type CLI text files was joined to a point shapefile.

The LLI text file from FRAGSTATS was also joined to another point shapefile so that there is one row per MODIS pixel. LLI reveals the general landscape structure. For example, for the largest patch index, the value for the largest patch in the pixel regardless of vegetation type is shown—savanna/long fallow with 9% for MODIS pixel 1 (Table 3).

TABLE 3. FRAGSTATS Results for Landscape-Level Indices

| Tile ID | Largest patch index | Patch richness | Split index | Patch density |
|---------|---------------------|----------------|-------------|---------------|
| 1       | 9%                  | 3              | 75.18       | 12.23         |
| 2       | 15%                 | 4              | 32.67       | 36.71         |

Statistical Test

Medians of fire regime measures (average frequency, variability of fires) were compared between vegetation types using Mann-Whitney test due to non-normal (skewed) distribution (Wilcoxon 1945; Mann and Whitney 1947). To examine normality of the data, Skewness-Kurtosis test was used (D’Agostino et al 1990; Royston 1991).

## CHAPTER 3

### RESULTS

This research examined the impact of vegetation type and landscape structure on fire regime at 500 m pixel resolution. Effects of changes in CLIs on fire regime variables (average burned dates, frequency, and standard deviation of burned dates) were assessed to understand how landscape structure and vegetation types affect the fire regime; LLIs were used to understand the effect of the general landscape structure on the fire regime.

#### Comparing average burned dates from Landsat and MODIS

Average burn date enabled detection of the temporal nature of burning across the savanna, as well as how the burned date manifests in different datasets. In Figure 5, descriptive statistics of average burned date by dataset are graphed. A boxplot splits the data into quartiles from the first quartile, median, to the third quartile. Two vertical lines, extending from the bottom and top of the box, show the smallest average burned date from the first quartile and the largest average burned date from the third quartile. When the data are skewed ( $p < 0.001$  of Skewness-Kurtosis test), median is preferred over mean. Landsat had the earliest average burned dates across pixels (median Jan 1), followed by MODIS active fire (Jan 8,  $p < 0.001$ ) and MODIS burned area (Jan 18,  $p < 0.001$ ). The dotted lines linking 25<sup>th</sup>, 50<sup>th</sup> (median), 75<sup>th</sup>, and 95<sup>th</sup> percentile values across datasets clearly show this tendency.

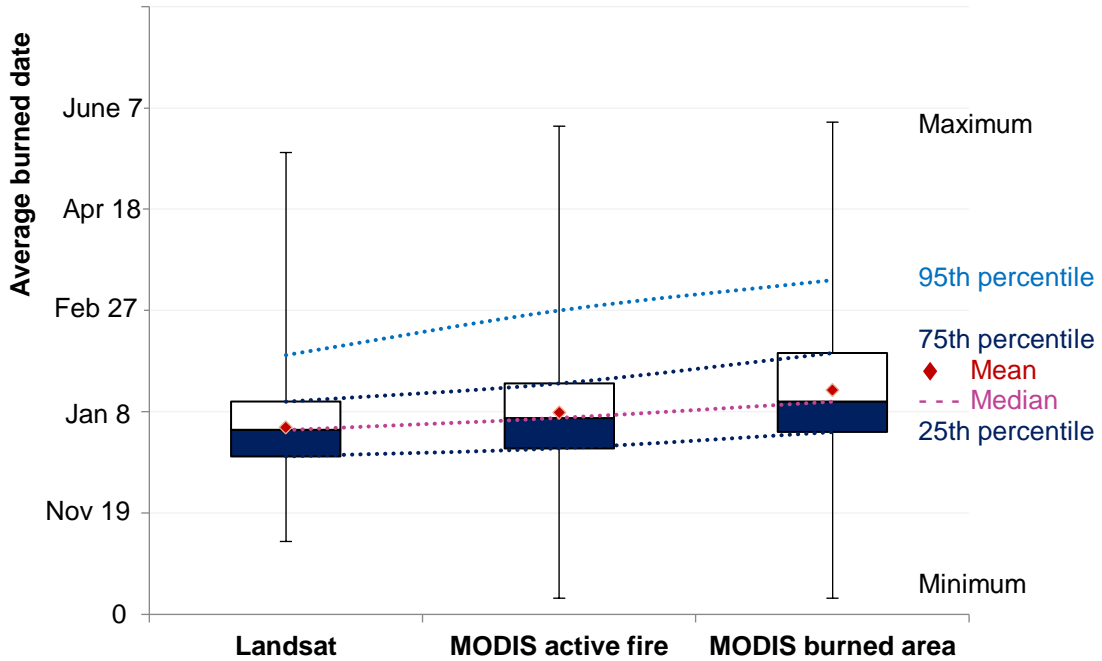


FIGURE 5. Box plots of burned dates (500 m pixel) by dataset

Note: During the 11-year study period, a total of 109,905 MODIS pixels had at least one land-cover type and one burned date (Landsat, MODIS burned area, or MODIS active fire) per pixel.

### Landsat Fire Regime

To visualize characteristics of the fire regime, boxplots by vegetation type are presented in Figures 6, 7, and 8, for average burned date, frequency of fires, and variability of average burned dates, respectively. Frequency describes the amount of times a pixel burned (a pixel could burn a maximum of 3 times—one per year). The standard deviation (SD) represents the overall variability between burned dates over the three years.

Figure 6-A compares the distribution of the average burned date between two areas: area with lower percentage cover of short grass (1<sup>st</sup> quartile) vs. area with higher

percentage cover (4<sup>th</sup> quartile). In areas with more short grass savanna (higher percentage cover), fires (median December 16) tended to occur early, compared to January 9 in the area with less short grass savanna ( $p < 0.05$ ).

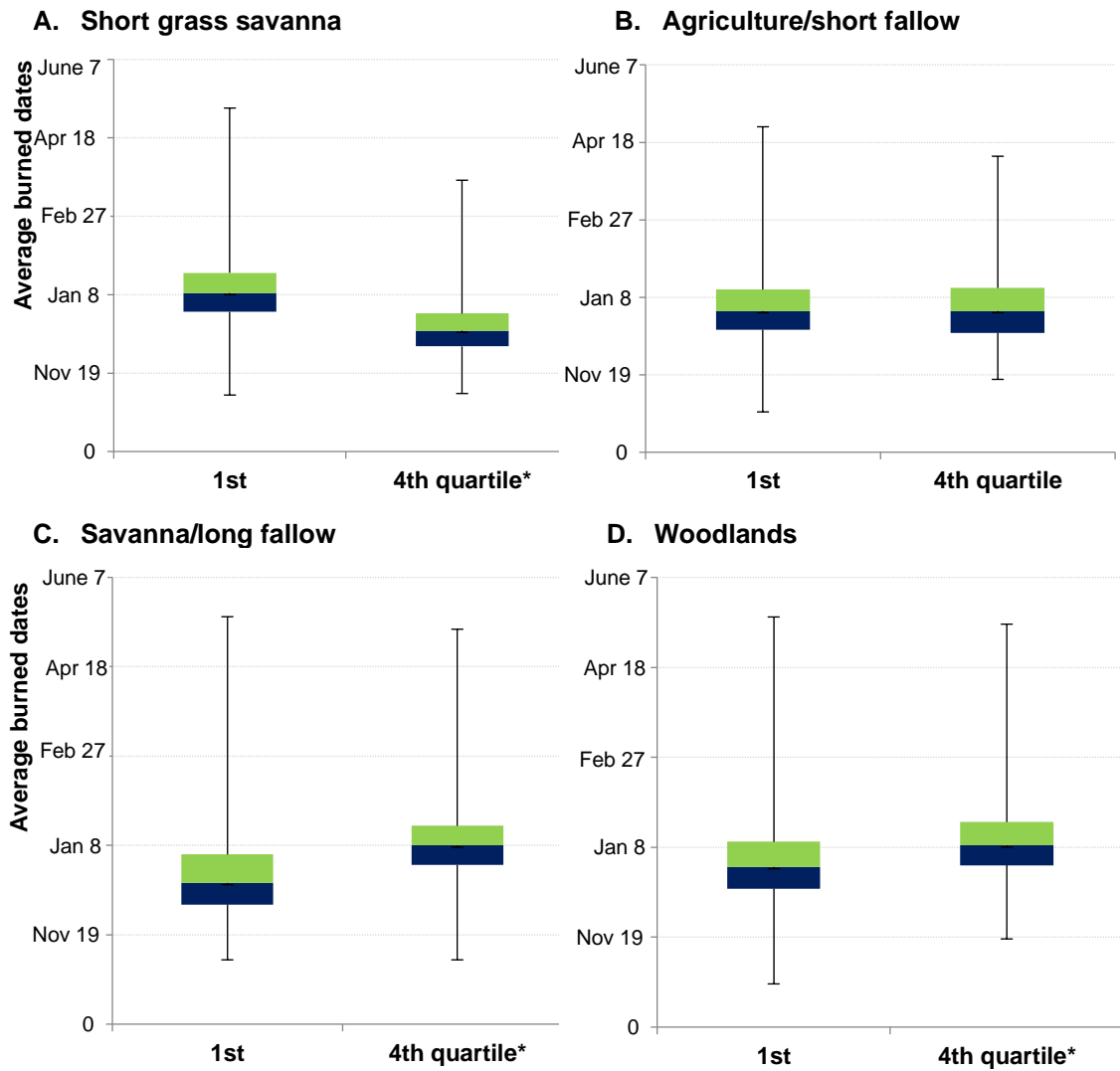


FIGURE 6. Box plots of average burned dates for 1<sup>st</sup> and 4<sup>th</sup> quartile of percentage cover of (a) short grass savanna, (b) agriculture/short fallow, (c) savanna/long fallow, and (d) woodlands.

\* indicates statistical difference in average burned dates between lower and upper quartile at a 5% level of significance based on Mann-Whitney test.

For agriculture/short fallow, average burned dates are not statistically different by proportion of agriculture/short fallow in the resolution of a MODIS pixel ( $p=0.11$ , Figure 6-B). Fires were likely to be later in areas with higher percentage of savanna/long fallow (median January 8) and woodlands (January 9), compared to December 18 and December 28 in areas with lower percentage of each, respectively, at a 5% level of statistical significance.

Over the 11-year period (three seasons) associated with the Landsat data, burning occurred 234 times in areas with higher percentage of short grass savanna, compared to 157 times in areas with lower percentage ( $p<0.001$ ; Figure 7A).

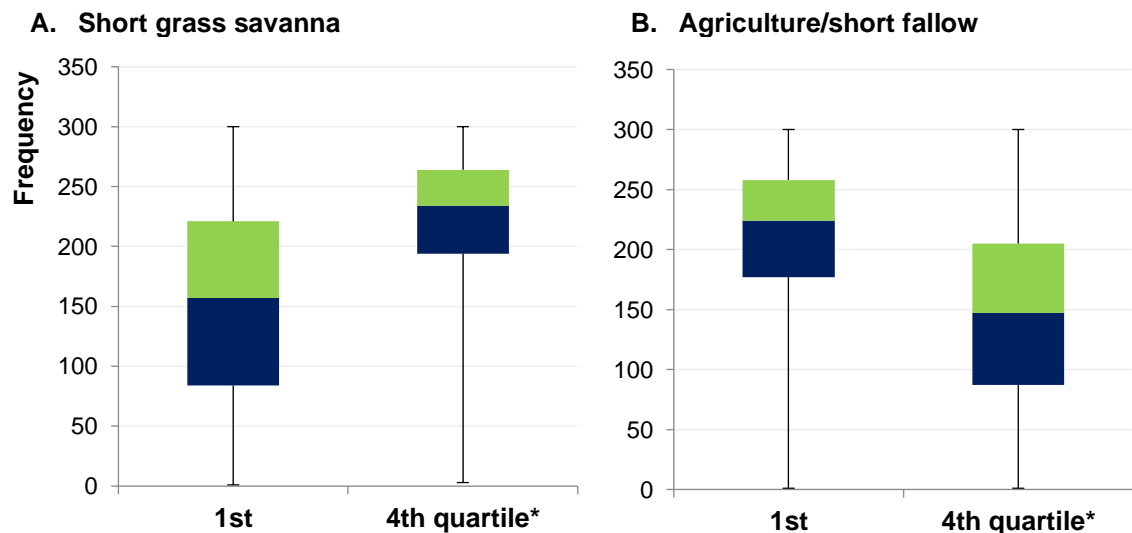


FIGURE 7a-b. Box plots of burn frequency for 1<sup>st</sup> and 4<sup>th</sup> quartile of percentage cover of (a) short grass savanna and (b) agriculture/short fallow

\* indicates statistical difference in frequency between lower and upper quartile at a 5% level of significance based on Mann-Whitney test.

Areas with higher percentage of agriculture/short fallow burned less frequently: (147 vs. 224 times,  $p < 0.001$ ), while areas with high percentage of savanna/long fallow burned more frequently (218 vs. 164 times,  $p < 0.001$ ). In woodlands, fires occurred more frequently over three seasons (201 vs. 196 times,  $p < 0.001$ ).

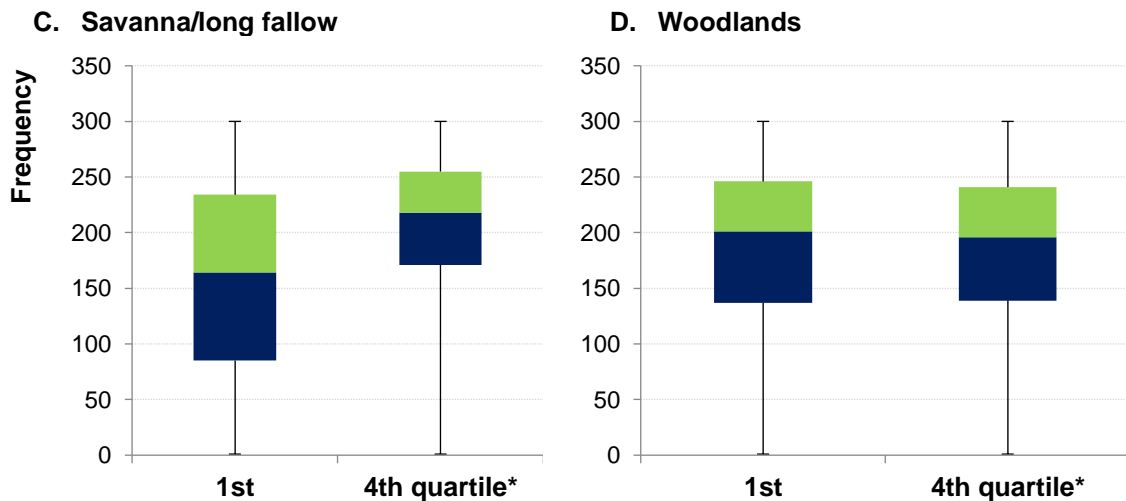


FIGURE 7c-d. Box plots of frequency of fires for 1<sup>st</sup> and 4<sup>th</sup> quartile of percentage cover of (c) savanna/long fallow and (d) woodlands  
\* indicates statistical difference in frequency between lower and upper quartile at a 5% level of significance based on Mann-Whitney test.

To see the variability of burned dates by vegetation type, one can check the vertical distance between the smallest and largest SD, rather than median value of SD (Figure 8). In areas with higher percentage of short grass and savanna-long fallow, fires spread within 91 to 94 days, compared to 101 to 102 days in areas with lower percentage; this difference indicates fires that were more regular.

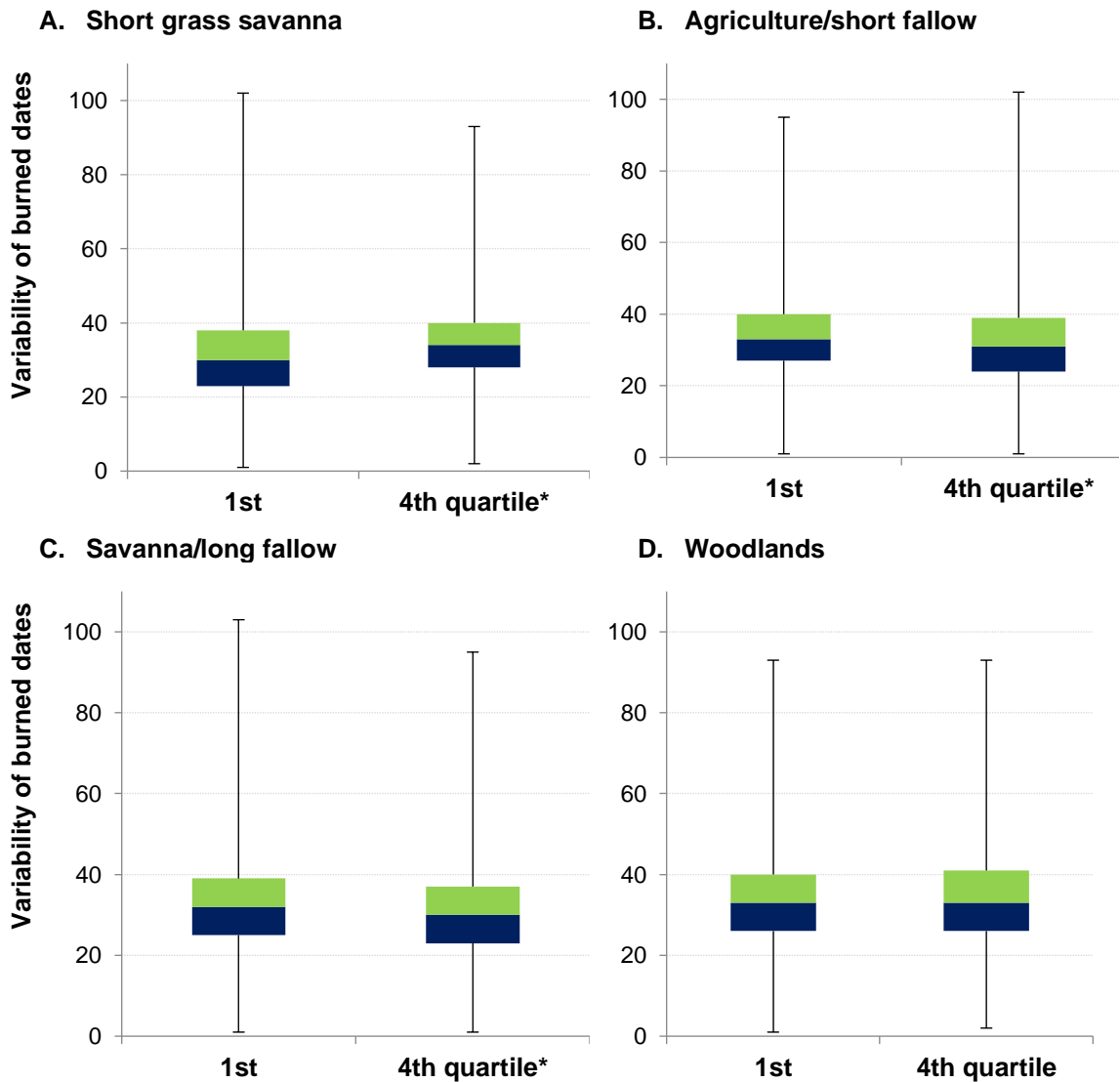


FIGURE 8. Box plots of variability of burned dates for 1<sup>st</sup> and 4<sup>th</sup> quartile of percentage cover of (a) short grass savanna, (b) agriculture/short fallow, (c) savanna/long fallow, and (d) woodlands.

\* indicates statistical difference in SD between lower and upper quartile at a 5% level of significance based on Mann-Whitney test.

Areas with higher percentage of agriculture/short fallow (upper quartile) showed the opposite tendency: fires that were less regular (range of 101 vs. 94). For woodlands,

there were no differences in variability of burned dates regardless of percentage of cover area.

The combined findings in Figures 6, 7, and 8 indicate that 1) short grass savanna burned more consistently and frequently earlier in the season; 2) agriculture/short fallow burned less consistently and frequently, but showed little difference in median value of average burned date; 3) in areas of savanna/long fallow, late fires tended to be more regular and frequent; and 4) in areas with woodlands, late fires tended to be more frequent. This analysis of Landsat data demonstrates the relative difference in timing and variability of burned dates, as well as frequency of fires, by vegetation type.

#### Landscape Indices

Descriptive statistics for CLI by vegetation type and LLI (Table 4) depict the full range of values for these indices across the entire study area:

*Proportion of area:* Savanna/long fallow was the dominant vegetation type (median of 42%), followed by agriculture/short fallow (21%), short grass (18%), and woodlands (5%).

*Largest Patch Size:* Savanna/long fallow patches were larger (median of 34%) than patches of other vegetation types, while woodlands patches were smaller (3%).

*Patch Density:* Within a 500 m pixel, there were more agriculture/short fallow and short grass savanna patches than other vegetation types.

*Shape Index:* Woodlands were likely to have square-shaped patches (smallest shape index), while savanna/long fallow area were likely to have non-square-shaped (largest shape index) patches.

TABLE 4. Descriptive Statistics for Class-Level Indices

| Class-level indices                 | Median | Mean | Min | Max   |
|-------------------------------------|--------|------|-----|-------|
| Short grass savanna (N=100,970)     |        |      |     |       |
| Proportion of area (%)              | 18.0   | 24.5 | 1.0 | 100.0 |
| Shape index                         | 1.4    | 1.5  | 1.0 | 4.3   |
| Largest patch index (%)             | 10.0   | 19.8 | 1.0 | 100.0 |
| Patch density                       | 12.2   | 13.4 | 4.1 | 57.1  |
| Agriculture/short fallow (N=98,052) |        |      |     |       |
| Proportion of area (%)              | 21.0   | 23.9 | 1.0 | 98.0  |
| Shape index                         | 1.5    | 1.6  | 1.0 | 4.1   |
| Largest patch index (%)             | 11.0   | 17.4 | 1.0 | 98.0  |
| Patch density                       | 16.3   | 15.3 | 4.1 | 57.1  |
| Savanna/long fallow (N=108,469)     |        |      |     |       |
| Proportion of area (%)              | 42.0   | 42.2 | 1.0 | 100.0 |
| Shape index                         | 1.9    | 2.0  | 1.0 | 4.3   |
| Largest patch index (%)             | 34.0   | 36.5 | 1.0 | 100.0 |
| Patch density                       | 12.2   | 12.4 | 4.1 | 53.0  |
| Woodlands (N=69,293)                |        |      |     |       |
| Proportion of area (%)              | 5.0    | 9.8  | 1.0 | 100.0 |
| Shape index                         | 1.1    | 1.2  | 1.0 | 3.8   |
| Largest patch index (%)             | 3.0    | 7.3  | 1.0 | 100.0 |
| Patch density                       | 8.2    | 10.1 | 4.1 | 48.9  |

Note: These percentages were calculated for land-cover types that fell within each 500 m pixel (not across the entire study area).

Relationships between landscape indices and fire regime in the Landsat fire regime dataset (500 m resolution) were evaluated. Pixels in the upper quartile range of a landscape index were compared to those in the lower quartile. Range was determined by each index. Burn date was classified as “early” (October to December) and “late” (January to May). This burn date classification was used to stratify the landscape index quartiles for comparison purposes, and to illustrate patterns. Note that Figures 9A, 10A, 11A, and 12A are maps on which Figure 5 is depicted.

Areas with a high proportion of *short grass savanna* were characterized by fewer (patch density) large (largest patch index) non-square (shape index) patches, with fires occurring earlier in the season and more frequently (Figure 9).

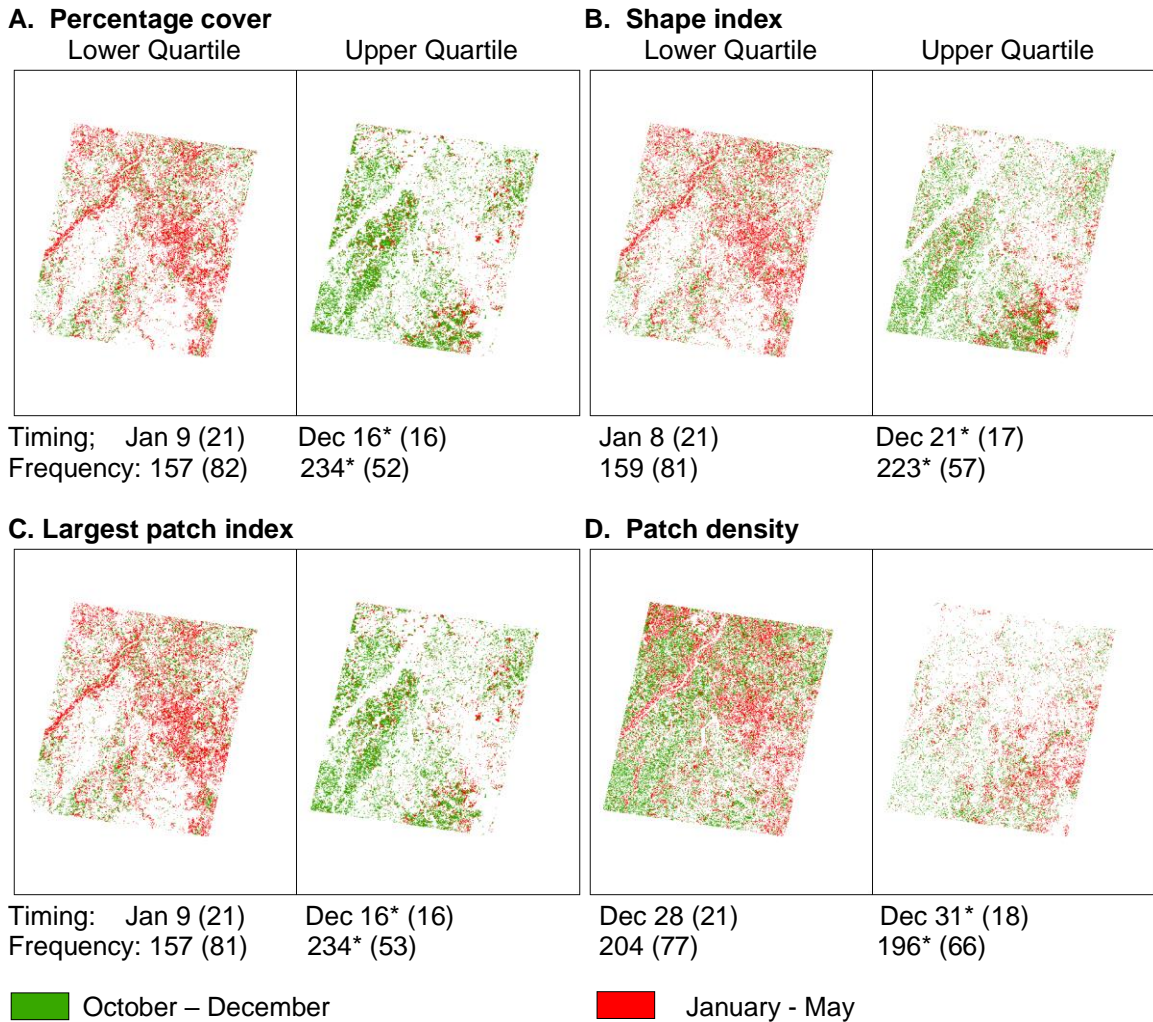


FIGURE 9. Short grass savanna. Lower and upper quartiles of (a) percentage cover, (b) shape index, (c) largest patch index, and (d) patch density. Median (SD). Areas with more irregular, non-square-shaped short grass savanna patches (9b) had an 18-day earlier average burned date (median of Dec. 21) than more square-shaped patches (median of Jan. 8). Larger patches (9c) tended to burn 24 days earlier (Dec. 16) compared with smaller patches, which tended to burn later (Jan. 9). Short grass savanna areas with smaller patch density (9d) burned 3 days earlier (Dec. 28), compared to areas with many patches (Dec. 31). \* represents a 5% level of significance.

Areas with a high proportion of *agriculture/short fallow* were likely to have many patches (patch density), with fires occurring earlier in the season, but less frequently than in areas with fewer patches (Figure 10).

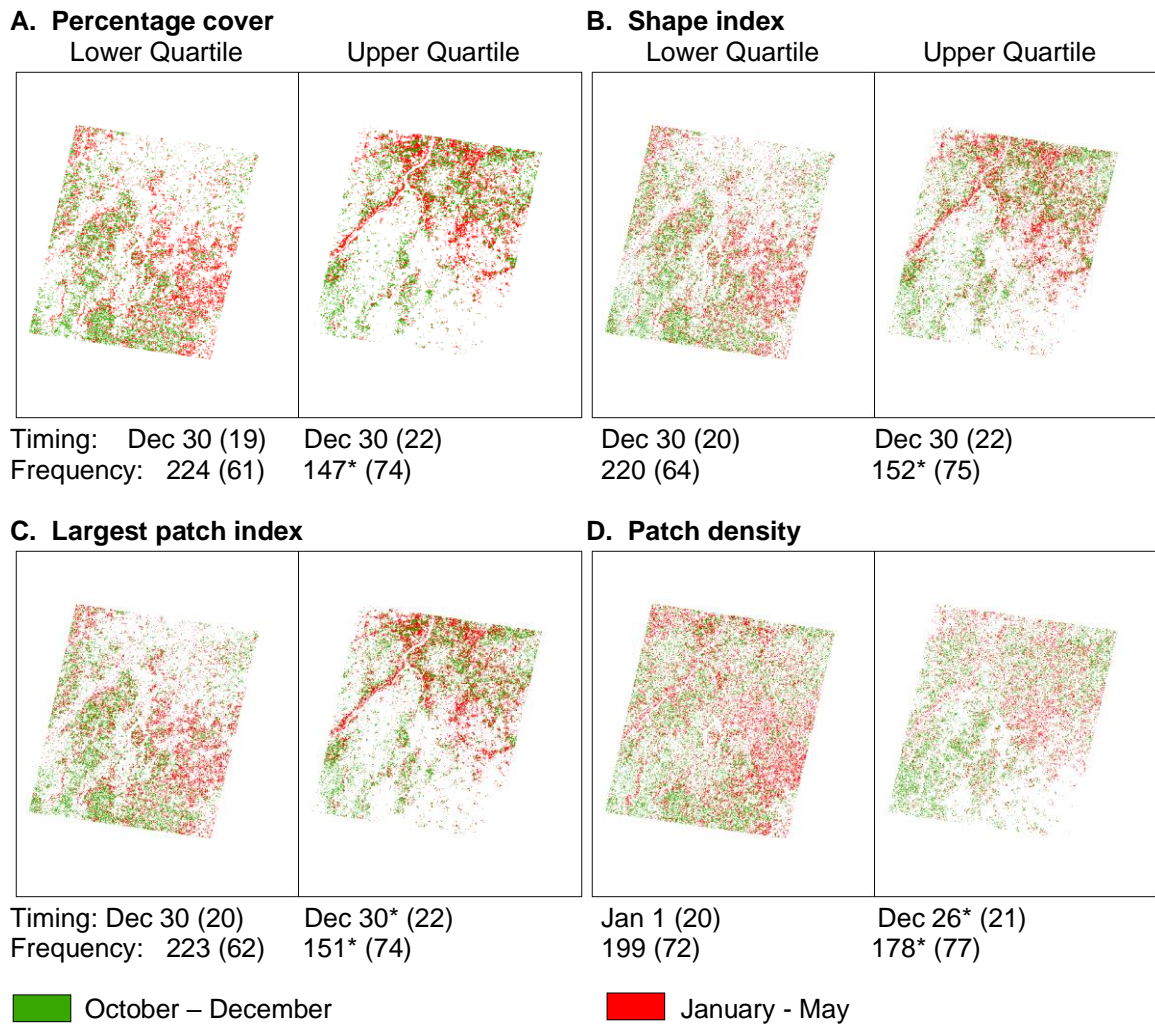


FIGURE 10. Agriculture/short fallow. Lower and upper quartiles of class level indices. Median (SD).

Agriculture/short fallow areas with many patches (10d) burned 6 days earlier (median of Dec. 26), compared to areas with few patches (Jan. 1). \* indicates that average burned date and frequency of fires are different between the upper and lower quartile for the largest patch and patch density indices at a 5% level of significance based on the Mann-Whitney test.

Areas with a high proportion of *savanna/long fallow* were likely to have fewer (smaller patch density), larger (patch index), non-square (shape index) patches, with fires occurring later in the season and more frequently (Figure 11).

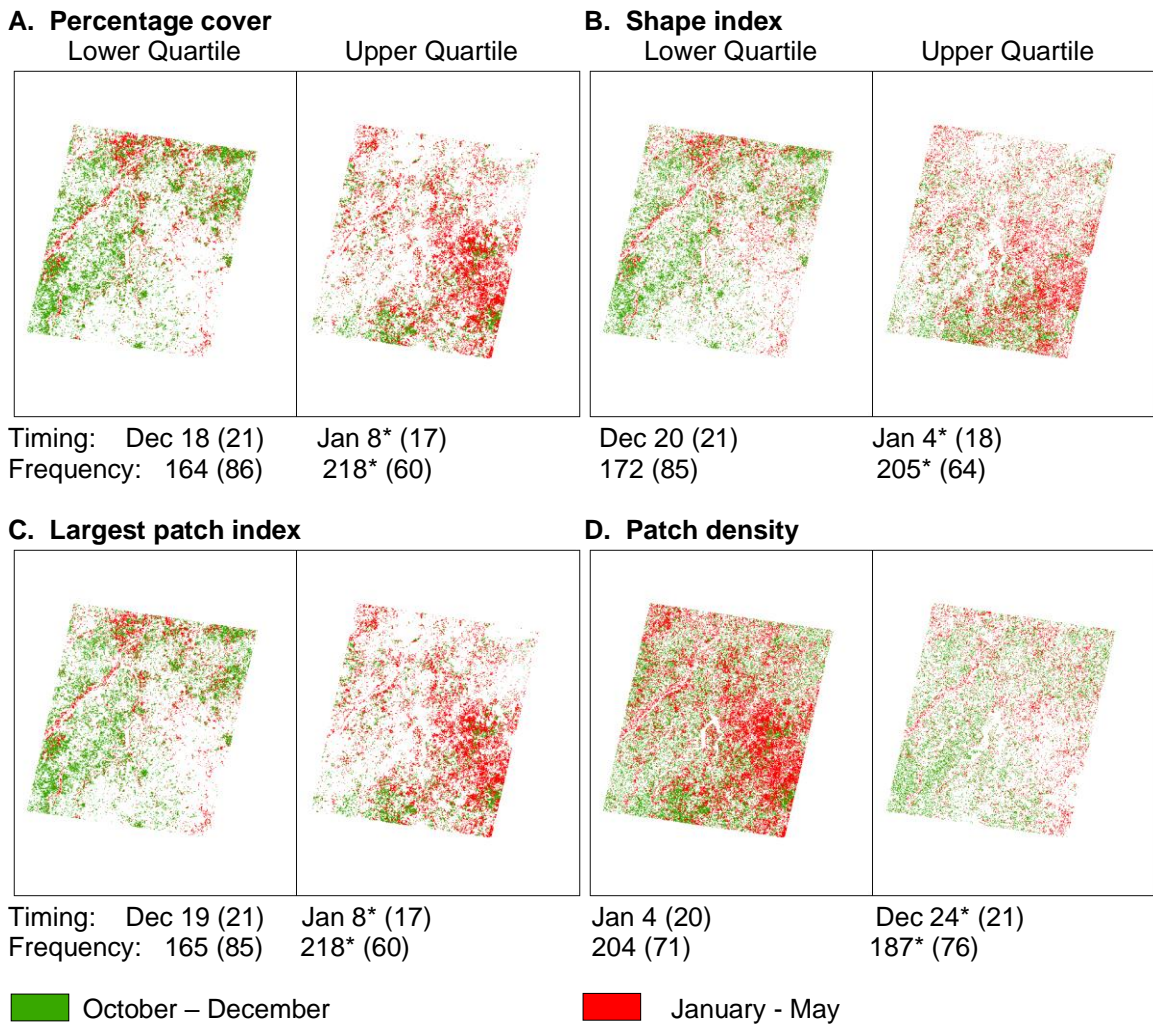


FIGURE 11. Savanna/long fallow. Lower and upper quartiles of class level indices. Median (SD).

Areas with more irregular, non-square shaped patches (11b) had a 15-day later average burned date (median of Jan. 4) than more regular-shaped patches (Dec. 21). Larger patches (11c) tended to burn 20 days later (median of Jan. 8) than smaller patches, which tended to burn earlier (Dec. 19). Savanna/long fallow areas with smaller patch density (11d) burned 15 days later (Jan. 4) than areas with many patches (median of Dec. 24). \* represents a 5% level of significance.

Areas with a high proportion of *woodlands* were likely to have many, larger, non-square patches, with fires occurring later in the season and less frequently than in areas with a lower proportion of woodlands (Figure 12).

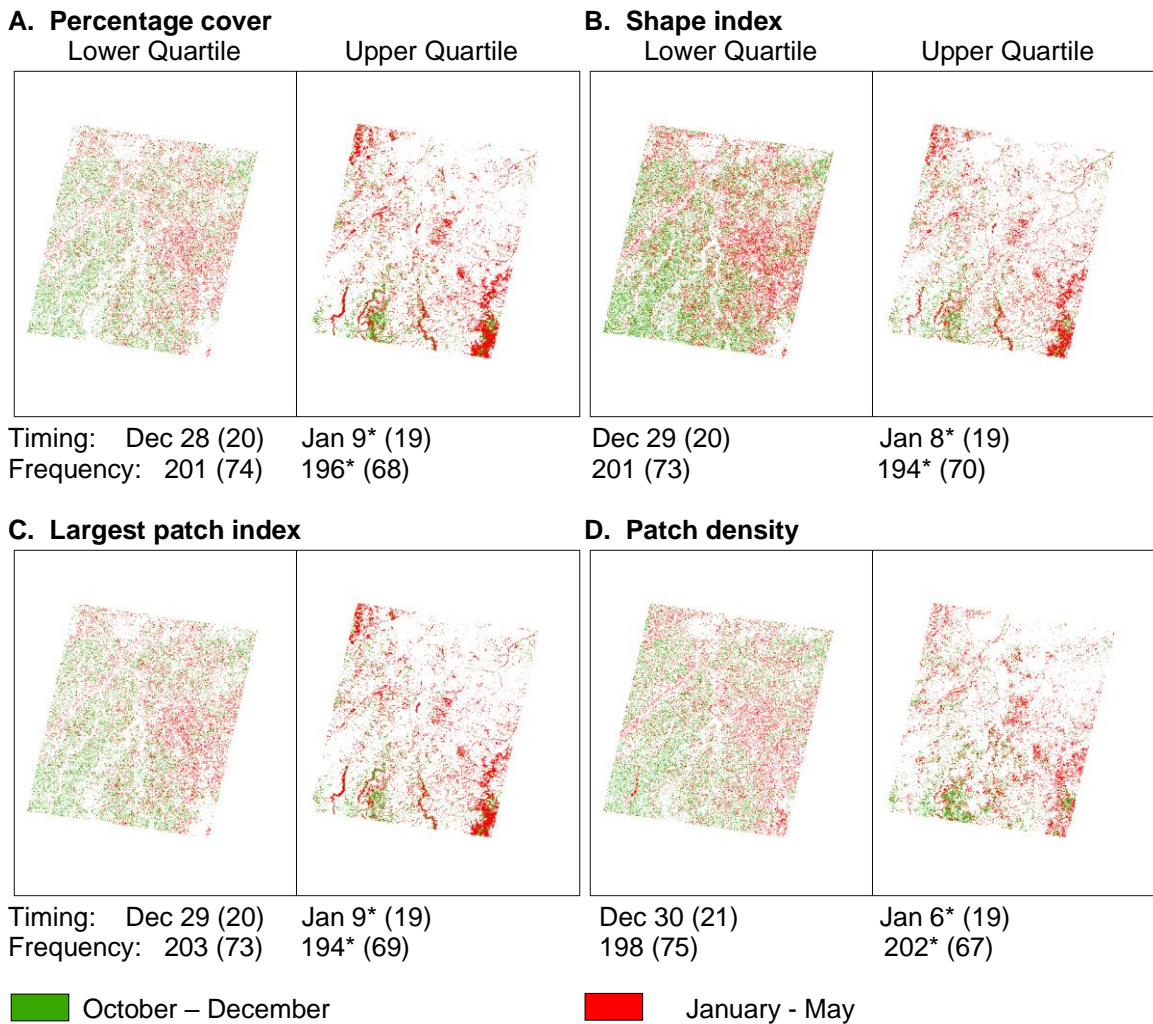


FIGURE 12. Woodlands. Lower and upper quartiles of class level indices. Median (SD).

Areas with a larger percentage cover of woodlands (12a) had a 12-day later average burned date (January 9) than areas with a lower proportion of woodlands (median of Dec. 28). Areas with more irregular, non-square-shaped woodlands patches (12b) had a 10-day later average burned date (Jan. 8). Larger patches (12c) tended to burn 11 days later (median of Jan. 9) than smaller woodlands patches (Dec. 29). Woodlands areas with higher patch density (12d) burned 7 days later (Jan. 6), compared to areas with few patches (Dec. 30). \* represents a 5% level of significance.

Compared to the spatial patterns per vegetation type (CLIs) depicted in Figures 9 through 12, the LLI (Figure 13) shows a more comprehensive and holistic view of the spatial pattern of vegetation types and temporal pattern of burn across the landscape.

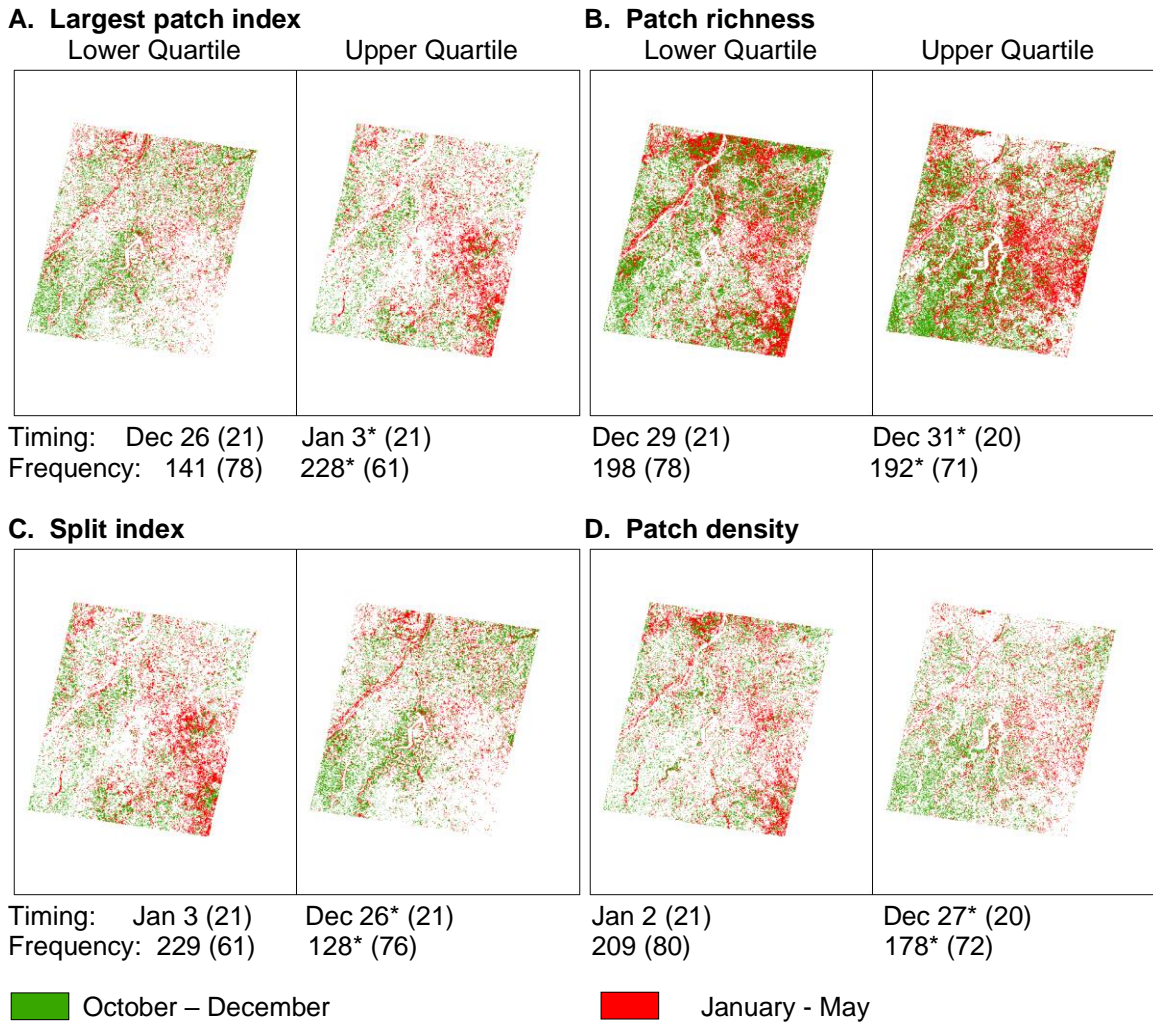


FIGURE 13. Landscape. Lower and upper quartiles of (a) largest patch index, (b) patch richness, (c) split index, and (d) patch density for landscape. Median (SD).

Areas with smaller patches (13a) and more fragmentation (13c) had an 8-day earlier average burned date (median of Dec. 26). Areas with fewer vegetation types (13b) had a 2-day earlier average burned date (Dec. 29). Areas with many patches (13d) had a 6-day earlier average burned date (Dec. 27). \* indicates that average burned dates and frequency of fires between the upper and lower quartile for each index are different at a 5% level of significance based on the Mann-Whitney test.

Early fires tended to be more fragmented and have smaller patches; thus, many small fires burned in areas with fewer vegetation types (three) than late fires. Though specific vegetation types are not called out in the LLI analysis, it is likely from the CLI results that these vegetation types consisted of short grass savanna, agriculture/short fallow and savanna/long fallow. Early fires in the LLI tended to burn less frequently (smaller frequency values). In the CLI analysis, late large fires were associated with savanna/long fallow and woodlands. Late fires in the LLI were associated with larger patches, and burned all four vegetation types (patch richness). In the CLI analysis, late large fires were associated with savanna/long fallow and woodlands.

## CHAPTER 4

### DISCUSSION

The study is driven by four key research questions: (1) how does landscape pattern affect the fire regime in an African savanna? (2) do particular types of vegetation cover have unique effects on specific aspects of the fire regime? (3) which common landscape ecological indices have the most potential for linking land cover and fire regime? (4) what potential do landscape indices offer for resolving the issue of scale in use of coarse-resolution fire and land-cover data? This study finds that landscape pattern affects the fire regime in the savanna of Mali. Laris (2005) showed that mosaic fire regimes in Mali have a distinct temporal component: early fires tended to be smaller and more fragmented than later fires. As confirmed here, early fires do tend to be fragmented and small, and more numerous than late fires in areas with fewer vegetation types.

At the landscape level, findings show that early fires were associated with a decrease in the largest patch index (smaller patches) and the patch richness index (less diverse vegetation type), as well as an increase in the splitting index (smaller patches) and the patch density (many patches). The data indicate that earlier fires were associated with landscape heterogeneity and fragmentation, but not necessarily a higher diversity of vegetation types. In other words, a landscape composed of a few vegetation types (including short grass savanna), highly fragmented with small patches of vegetation, burned earliest. Conversely, areas that have little fragmentation and large, homogenous

patches of vegetation burned later. In western Burkina Faso, Caillault et al. (2014) reported that fires were clustered spatially, based on temporal proximity between fires, and that the fire regime showed a regular pattern in a fire season.

Because these studies did not examine landscape pattern, this study shows how landscape pattern influences the fire regime. This is thus a novel finding, confirming that pattern affects process: specifically, vegetation landscape patterns affect the fire regime.

Fire timing and frequency varied by vegetation type. The results indicate that fires occurred earliest in short grass savanna, followed by agriculture/short fallow, savanna/long fallow, and woodlands. These findings are consistent with seasonal changes in fuel moisture levels in the vegetation and with human burning practices. As Laris (2002, 2011) has argued, short, annual grasses have faster desiccation rates in southern Mali than other vegetation types. For this reason, people set early fires in short grass areas with the goal of fragmenting the landscape to prevent large and damaging fires. This preventive practice results in a burning regime that creates a more fragmented pattern. Areas under long fallow cycles, characterized by more perennial grasses and denser woody vegetation, can hold moisture longer than areas of short fallow, composed primarily of annual grasses. Long fallow savanna patches have non-square shapes and larger-sized patches. Late fires in patches of savanna/long fallow area thus spread and burn in a larger, more contiguous pattern.

Further, the results indicate that landscape heterogeneity by vegetation type plays a critical role in determining the timing and frequency of fire. Few, large, and non-square-shaped patches were associated with earlier burned dates in short grass savanna areas; in savanna/long fallow areas, these same patterns were associated with later burned

dates. In woodlands, where there were many and smaller irregularly-shaped patches, fires occurred at later dates. In agriculture/short fallow areas, many patches were associated with earlier burn dates. Fires burned more frequently in savanna/long fallow or short grass savanna where there were larger and fewer patches with irregular shapes.

Prior studies examining a relationship between landscape variables and fire regime have not fully accounted for the nature of burned-area data. Burned-area sample units (a MODIS pixel for this study) below the level of a single fire are not spatially independent, owing to the contiguous spread of fires through the landscape (Moreno et al 2011). Further, fires are temporally and spatially correlated (Chou et al 1990). Consequently, the assumption of independence between two neighboring landscape sampling units is inappropriate (Dasgupta and Alldredge 2002). To better capture relationships between landscape characteristics and fire regime dynamics, this study used landscape indices to consider elements within a 500 m block (a MODIS pixel) as related or spatially dependent.

Research methods informed the four main questions about the effect of landscape pattern on fire regime. With Landsat resolution degraded to 500m, neighboring burned pixels (30m) within a 500m pixel were seen as spatially dependent and it was possible to analyze spatial patterns formed by the 30m pixels (i.e., size and shape of each patch formed by the burned pixels, distribution of patches, and number of patches in a 500 m pixel). This detailed information about burn scar patterns was combined with temporal patterns from three datasets with different resolutions to evaluate effects of vegetation landscape pattern on fire regime.

A few recent studies regarded landscape indices in studying fires patterns or regimes. In Spain, Loepfe et al (2010) found homogeneity and land-cover type important. They used landscape indices to analyze interactions between landscape patterns and wildfires, finding that fire spread is facilitated by high fuel load, use/cover types, and homogeneous terrains, and that fire promotes landscape homogeneity. Lentile et al. (2005) used FRAGSTATS to estimate landscape indices in the Black Hills of South Dakota, examining spatial patterns of burn severity at the landscape level after the 2000 Jasper fire. They found that mixed-severity fire, in conjunction with frequent surface fire, played an important role in shaping the area's forest structure, a spatially heterogeneous ponderosa pine forest.

Compared to other studies on landscape pattern and fire, this Mali study is unique in that it examines the effect of landscape characteristics on fire timing, frequency, and variability. Findings indicate that fragmentation and size and shape of patches (which differ in vegetation type), are important factors affecting the timing and frequency of fires. The findings reaffirm the hypothesis put forth by Laris (2011): that vegetation cover in a savanna determines fire regime, not the converse as has long been argued in the literature (e.g., Aubreville 1949; Louppe et al 1995; Furley 2008).

Coarse-resolution MODIS data had later burned date estimates than Landsat estimates. Coarse-resolution data tended to overestimate large fires, which burned later, and to underestimate small fires that burned early in the season (Laris 2005; Eva and Lambin 1998). Small fires were undetected by MODIS burned area because they did not cover enough of a 500 m pixel to reach the detection threshold. In comparison, MODIS active fire could detect small fires by using the thermal band to detect heat emitted by

fires in a 1 km pixel. Thus, burned date range from MODIS active fire is closer to Landsat burned dates than MODIS burned area range. Although MODIS active fire data do show more information on pattern and timing of fires than MODIS burned area, they still tended to miss small, early fires that burned quickly and had short residence times.

Results may be influenced also by inevitable modifiable aerial unit problem (MAUP) in processing of remotely sensed data (Dark and Bram 2007). Because spatial and temporal constructs are defined by the data collectors (Landsat and MODIS), the spatial and temporal structures of the datasets influence our perception of the landscape, and may also influence the associated aggregation, disaggregation and resampling methods used. The nature and extent of this impact is unknowable.

Additionally, the findings need to be interpreted within the context of a dynamic relationship between landscape structure, fire regimes, and people's burning practices. For example, homogenous landscapes with high fuel loads and high connectivity are expected to favor high fire intensity and spread (Vega-García and Chuvieco 2006). In turn, fire in many landscapes tends to change land-cover types (Lloret et al 2002; Viedma et al 2006). In some cases, a fire may have reduced fuel load and connectivity, decreasing the probability of further fires and creating a negative feedback (Niklasson and Granström 2000; Stambaugh and Guyette 2008). In other cases, positive feedbacks may have been created by the high flammability of fuels that developed shortly after a fire (Vilà et al 2001); enhanced connectivity between burned areas (Vázquez and Moreno 2001; Viedma et al 2006); and reduction in landscape heterogeneity (Lloret et al 2002; Stambaugh and Guyette 2008; Viedma et al 2006). Interactions between a fire and a landscape often depended upon vegetation type (i.e., savanna differs from forest which

differs from Mediterranean scrublands), as well as how humans interacted with the landscape. Human activity becomes part of the dynamic of where fires occur and how they spread. The footprints of these fires influence patterns of vegetation and its regeneration, which in turn influence human land-use (Millington 2005; Laris 2013), and the relationship is a cycle.

## REFERENCES

- Agee J (1993) Fire ecology of Pacific Northwest forests Island Press, Washington, D.C.
- Archibald S, Roy DP, Van Wilgen BW, Scholes RJ (2009) What limits fire? An examination of drivers of burned area in sub-equatorial Africa. *Global Change Biology* 15:613-630
- Archibald S, Nickless A, Govender N, Scholes RJ, Lehsten V (2010) Climate and the inter-annual variability of fire in southern Africa: a meta-analysis using long-term field data and satellite-derived burned area data. *Global Ecology and Biogeography* 19:794–809
- Bajocco S, Ricotta C (2008) Evidence of selective burning in Sardinia (Italy): which land-cover classes do wildfires prefer? *Landscape Ecology* 23:241–248
- Bond WJ, Keeley JE (2005) Fire as a global ‘herbivore’: the ecology and evolution of flammable ecosystems. *Trends in Ecology and Evolution* 20:387-394
- Bond WJ, Woodward FI, Midgley GF (2005) The global distribution of ecosystems in a world without fire. *New Phytologist* 165:525–38
- Boschetti L, Flasse SP, Brivio PA (2004) Analysis of the conflict between omission and commission in low spatial dichotomic thematic products: The Pareto Boundary. *Remote Sensing of Environment*, 91, 280–292
- Boschetti L, Roy DP (2009) Strategies for the fusion of satellite fire radiative power with burned area data for fire radiative energy derivation. *Journal of Geophysical Research-Atmospheres*, 114 (D20)
- Boschetti L, Roy D, Hoffmann A, Humber M (2013) MODIS collection 5 burned area product—MCD45 user’s guide version 3.0.1, University of Maryland: College Park, MD, USA
- Brown TJ, Hall BL, Westerling AL (2004) The impact of twenty-first century climate change on wildland fire danger in the western United States: an applications perspective. *Climatic Change* 62:365-388

- Caillault S, Ballouche A, Delahaye D (2014) Where Are the ‘Bad Fires’ in West African Savannas? Rethinking Burning Management through a Space–Time Analysis in Burkina Faso. [online] *The Geographical Journal*. URL: <http://onlinelibrary.wiley.com/journal/10.1111/%28ISSN%291475-4959/earlyview>. DOI: 10.1111/geoj.12074
- Chou YH, Minnich RA, Salazar LA, Power JD, Dezzani RJ (1990) Spatial autocorrelation of wildfire distribution in the Idyllwild quadrangle, San Jacinto Mountain, California. *Photogrammetric Engineering and Remote Sensing* 56:1507–1513
- Christensen NL (1985) Shrubland fire regimes and their evolutionary consequences. In: Pickett STA, White P (eds) *The ecology of natural disturbance and patch dynamics*. Academic Press, Orlando, pp. 85–100.
- Cumming SG (2001) Forest type and wildfire in the Alberta boreal mixed wood: what do fires burn? *Ecological Applications* 11:97–110
- D’Agostino RB, Belanger A, D’Agostino RB Jr (1990) A Suggestion for Using Powerful and Informative Tests of Normality. *American Statistician* 44:316-321
- Dark SJ, Bram D (2007) The modifiable areal unit problem (MAUP) in physical geography. *Progress in Physical Geography* 31(5):471–479
- Dasgupta N, Alldredge JR (2002) A single-step method for identifying individual resources. *Journal of Agricultural Biological & Environmental Statistics* 7:208–221
- Duncan BW, Schmalzer PA (2004) Anthropogenic influences on potential fire spread in a pyrogenic ecosystem of Florida. *Landscape Ecology* 19:153-165
- Duvall CS (2011) Biocomplexity from the ground up: Vegetation patterns in a West African savanna landscape. *Annals of the Association of American Geographers* 101:497–522
- ESRI (2009) ArcGIS online world Imagery Basemap. Esri, Redlands, CA
- Eva H, Lambin EF (1998) Remote sensing of biomass burning in tropical regions: Sampling issues and multisensor approach. *Remote Sensing of Environment* 64:292–315
- Furley PA, Rees RM, Ryan CM, Saiz G (2008) Savanna burning and the assessment of long-term fire experiments with particular reference to Zimbabwe. *Progress in Physical Geography* 32: 611–634

- Giglio L, Descloitres J, Justice CO, Kaufman YJ (2003) An enhanced contextual fire detection algorithm for MODIS. *Remote Sensing of Environment* 87:273–282
- Giglio L (2007) Characterization of the tropical diurnal fire cycle using VIRS and MODIS observations. *Remote Sensing of Environment* 108:407–421
- Giglio L, Randerson J, Van der Werf G, Kasibhatla P, Collatz G, Morton D, DeFries R (2010) Assessing variability and long-term trends in burned area by merging multiple satellite fire products. *Biogeosciences* 7:1171–1186
- Jeltsch F, Weber G, Grimm V (2000) Ecological buffering mechanisms in savannas: A unifying theory of long-term tree–grass coexistence. *Plant Ecology* 150:161–171
- Keeley JE, Fotheringham CJ, Morais M (1999) Reexamining fire suppression impacts on brushland fire regimes. *Science* 284: 1829–1832
- Keeley JE, Zedler PH (2009) Large, high-intensity fire events in southern California shrublands: debunking the fine-grain age patch model. *Ecological Applications* 19:69–94
- Koppmann R, Von Czapiewski K, Reid J (2005) A review of biomass burning emissions, part I: Gaseous emissions of carbon monoxide, methane, volatile organic compounds, and nitrogen containing compounds. *Atmospheric Chemistry and Physics* 5:10455–10516
- Laris P (2002) Burning the Seasonal Mosaic: Preventative Burning Strategies in the Wooded Savanna of Southern Mali. *Human Ecology* 30: 155–186
- Laris P (2005) Spatiotemporal problems with detecting seasonal-mosaic fire regimes with coarse-resolution satellite data in savannas. *Remote Sensing of Environment* 99:412–24
- Laris P (2011) Humanizing savanna biogeography: linking human practices with ecological patterns in a frequently burned savanna of southern Mali. *Annals of the Association of American Geographers* 101:1067–1088
- Laris P (2013) Integrating Land Change Science and Savanna Fire Models in West Africa. *Land*, 2:609–636
- Lentile LB, Smith FW, Shepperd W D (2005) Patch structure, fire-scar formation, and tree regeneration in a large mixed-severity fire in the South Dakota Black Hills, USA. *Canadian Journal of Forest Research* 35:2875–2885
- Littell JS, McKenzie D, Peterson DL, Westerling AL (2009) Climate and wildfire area burned in western U.S. ecoregions, 1916–2003. *Ecological Applications* 19:1003–1021

- Lloret F, Calvo E, Pons X, Díaz-Delgado R (2002) Wildfires and landscape patterns in the East European Peninsula. *Landscape Ecology* 17:745–759
- Loepfe L, Martínez-Vilalta J, Oliveres J, Piñol J, Lloret F (2010) Feedbacks between fuel reduction and landscape homogenisation determine fire regimes in three Mediterranean areas. *Forest Ecology and Management* 259:2366–2374
- Loepfe L, Martínez-Vilalta J, Piñol J (2011) An integrative model of human influenced fire regimes and landscape dynamics. *Environmental Modelling and Software* 26:1028–1040
- Louppe D, Oattara N, Coulibaly A (1995) The effects of brush fires on vegetation: The Aubréville Fire Plots after 60 years. *Commonwealth Forestry Review* 74:288–291
- Lutz JA, van Wagendonk JW, Thode AE, Miller JD, Franklin JF (2009) Climate, lightning ignitions, and fire severity in Yosemite National Park, California, USA. *International Journal of Wildland Fire* 18:765–774.
- Mann HB, Whitney DR (1947) On a test of whether one of two random variables is stochastically larger than the other. *Annals of Mathematical Statistics* 18:50–60
- Martínez J, Vega-García C, Chuvieco E (2009) Human caused wildfire risk rating for prevention planning in Spain. *Journal of Environmental Management* 90:1241–1252
- McGarigal K, Cushman SA, Ene E (2012) FRAGSTATS v4: Spatial pattern analysis program for categorical and continuous maps. Computer software program produced by the authors at the University of Massachusetts, Amherst. Available at the following web site:  
<http://www.umass.edu/landeco/research/fragstats/fragstats.html>
- McGarigal K (2015) FRAGSTATS help. University of Massachusetts, Amherst
- Mermoz M, Kitzberger T, Veblen TT (2005) Landscape influences on occurrence and spread of wildfires in Patagonian forests and shrublands. *Ecology* 86:2705–2715
- Midha N, Mathur PK (2010) Assessment of forest fragmentation in the conservation priority Dudhwa landscape, India using FRAGSTATS computed class level metrics. *Journal of the Indian society of Remote Sensing* 38:487–500
- Millington JDA (2005) Wildfire risk mapping: considering environmental change in space and time. *Journal of Mediterranean Ecology* 6:33–42

- Minnich R (1983) Fire mosaics in southern California and northern Baja. *California Science* 21: 1287–94
- Minnich RA (2001) An integrated model of two fire regimes. *Conservation Biology* 15: 1549–1553
- Moreira F, Rego FC, Ferreira PG (2001) Temporal (1958–1995) pattern of change in a cultural landscape of north-western Portugal: implications for fire occurrence. *Landscape Ecology* 16:557–567
- Moreira F, Vaz P, Catry F, Silva JS (2009) Regional variations in wildfire susceptibility of land-cover types in Portugal: implications for landscape management to minimize fire hazard. *International Journal of Wildland Fire* 18:563–574
- Moreno JM, Viedma O, Zavala G, Luna B (2011) Landscape variables influencing forest fires in central Spain. *International Journal of Wildland Fire* 20:678–689
- Moritz MA (2003) Spatiotemporal analysis of controls on shrubland fire regimes: age dependency and fire hazard. *Ecology* 84:351–361
- Moritz MA, Keeley JE, Johnson EA, Schaffner AA (2004) Testing a basic assumption of shrubland fire management: does the hazard of burning increase with the age of fuels? *Frontiers in Ecology and the Environment* 2:67–72
- Nasi R, Sabatier M (1988) *Projet Inventaire des ressources Ligneuses au Mali; Bamako* DNEF: Bamako, Mali
- Niklasson M, Granström A (2000) Numbers and sizes of fires: long-term spatially explicit fire history in a Swedish boreal landscape. *Ecology* 81:1484–1499
- Nunes MCS, Vasconcelos MJ, Pereira JMC, Dasgupta N, Alldredge RJ (2005) Land cover type and fire in Portugal: do fires burn land cover selectively? *Landscape Ecology* 20:661–673
- Parr CL, Brockett BH (1999) Patch-mosaic burning: A new paradigm for savanna fire management in protected areas? *Koedoe* 42: 117–130
- Pausas JG, Fernandez-Munoz S (2012) Fire regime changes in the Western Mediterranean Basin: from fuel-limited to drought-driven fire regime. *Climatic Change* 110:215–226
- Pickett ST, White PS (1985) *The ecology of natural disturbance and patch dynamics*. Academic Press, New York, NY, USA

- Piñol J, Beven K, Viegas DX (2005) Modelling the effect of fire-exclusion and prescribed fire on wildfire size in Mediterranean ecosystems. *Ecological Modelling* 183:398–409
- Piñol J, Castellnou M, Beven KJ (2007) Conditioning uncertainty in ecological models: assessing the impact of fire management strategies. *Ecological Modelling* 207:34–44
- Raines GL (2002) Description and comparison of geologic maps with FRAGSTATS—a spatial statistics program. *Computers and Geosciences* 28:169-177
- Randerson JT, Chen Y, Van Der Werf GR, Rogers BM, Morton DC (2012) Global burned area and biomass burning emissions from small fires. *Journal of Geophysical Research: Biogeosciences* 117:G04012
- Roy DP, Boschetti L, Justice CO, Ju J (2008) The collection 5 MODIS burned area product — Global evaluation by comparison with the MODIS active fire product. *Remote Sensing of Environment* 112:3690–3707
- Royston JP (1991) Comment on sg3.4 and an Improved D’Agostino test. *Stata Technical Bulletin* 3:13-24
- Sá A, Pereira J, Charlton M, Mota B, Barbosa P, Fotheringham A (2010) The pyrogeography of sub-Saharan Africa: a study of the spatial nonstationarity of fire–environment relationships using GWR. *Journal of geographical systems* 13:227–248
- Sankaran M, Hanan N, Scholes R, Ratnam J, Augustine D, Cade B, Gignoux J et al (2005) Determinants of woody cover in African savannas. *Nature* 438:846–849
- Scholes R, Archer S (1997) Tree–grass interactions in savannas. *Annual Review of Ecology and Systematics* 28:517–44
- Schroeder W, Prins E, Giglio L, Csiszar I, Schmidt C, Morisette J et al (2008) Validation of GOES and MODIS active fire detection products using ASTER and ETM plus data. *Remote Sensing of Environment* 112:2711–2726
- Shang Z, He HS, Lytle DE, Shifley SR, Crow TR (2007) Modeling the long-term effects of fire suppression on central hardwood forests in Missouri Ozarks, using LANDIS. *Forest Ecology and Management* 242:776–790
- Smith AMS, Wooster MJ (2005) Remote classification of head and backfire types from MODIS fire radiative power and smoke plume observations. *International Journal of Wildland Fire* 14:249–254

- Stambaugh MC, Guyette RP (2008) Predicting spatio-temporal variability in fire return intervals using a topographic roughness index. *Forest Ecology and Management* 254:463–473
- Turner MG (1989) Landscape ecology: the effect of pattern on process. *Annual review of ecology and systematics* 20:171-197
- Vázquez A, Moreno JM (2001) Spatial distribution of forest fires in Sierra de Gredos (central Spain). *Forest Ecology and Management* 147:55–65
- Vega-Garcia C, Chuvieco E (2006) Applying local measures of spatial heterogeneity to Landsat-TM images for predicting wildfire occurrence in Mediterranean landscapes. *Landscape Ecology* 21:595–605
- Viedma O, Moreno JM, Rieiro I (2006) Interactions between land use/land cover change, forest fires and landscape structure in Sierra de Gredos (central Spain). *Environmental Conservation* 33, 212–222
- Vilá M, Lloret F, Ogheri E, Terradas J (2001) Positive fire–grass feedback in Mediterranean Basin woodlands. *Forest Ecology and Management* 147:3–14
- Wilcoxon F (1945) Individual comparisons by ranking methods. *Biometrics* 1:80–83